AN ABSTRACT OF THE THESIS OF

George D. Redden for the degree of Master Of Science

in Oceanography presented on September 3, 1982

Title: CHARACTERISTICS OF PHOTOCHEMICAL PRODUCTION OF CARBON MONOXIDE IN SEAWATER

Redacted for privacy

Abstract approved: _____
Dr. Louis I. Gordon

Rates of photochemical production of carbon monoxide were measured in seawater samples exposed to sunlight and fluorescent light. The effect of radiation wavelength was studied using cellulose acetate, Mylar, polycarbonate, and yellow acrylic filters to attenuate the middle and near ultraviolet (UV), and blue-green regions of the solar spectrum. The effect of more discrete wavebands was measured using spectra produced by various fluorescent lamp and filter combinations. It was found that radiation from 290 nm through at least 460 nm (blue light) was effective for producing CO. It appears that CO production increases exponentially with decreasing wavelength.

It was also found that CO production was linearly related to the integrated irradiance from sunlight and that production ceased when samples were removed from the light. This suggests that CO was produced by a relatively fast photochemical reaction. A simple model was used to demonstrate that the observed delay of peak CO concentrations in surface waters behind peak light levels could be explained assuming instantaneous production and instantaneous or

delayed consumption.

Production of CO in samples exposed to sunlight increased with increasing O_2 concentration although the rate of increase was less with higher O_2 concentrations. Significant CO was produced in the apparent absence of O_2.

Seawater with added acetone, acetaldehyde, and humic acid produced additional CO when irradiated by sunlight. Addition of humic acid resulted in approximately three orders of magnitude more CO per substrate weight than acetone or acetaldehyde. Samples treated with acetone and acetaldehyde also produced methane. Addition of urea, dextrose, and acetic acid had no measurable effect.

These experiments indicate that a possible mechanism for photochemical CO production is elimination of carbonyl functional groups from an undefined fraction of dissolved organic matter by carbon-carbonyl bond cleavage. Oxygen may photochemically oxidize organic matter thereby increasing the number of photo-reactive carbonyl groups.

CHARACTERISTICS OF PHOTOCHEMICAL PRODUCTION OF CARBON MONOXIDE IN SEAWATER

by

George Dean Redden

A THESIS

submitted to

Oregon State University

in partial fulfillment of
the requirements for the
degree of
Master of Science

Completed September 3, 1982

Commencement June, 1983

APPROVED:

Redacted for privacy

Associate Professor of Oceanography in charge of major

Redacted for privacy

Dean of School of Oceanography

Redacted for privacy

Dean of Graduate School

Date of thesis presentation September 3, 1982

Typed by George Dean Redden

ACKNOWLEDGMENTS

Primarily as a dedication, this thesis is for my parents, and Carol, my sister, who have put up with three years of wondering if I was still alive, and with visits that were all too short. Thanks for keeping your humor, understanding, and support through it all. So what if I was a little late?

Many thanks to Lou, my advisor, who provided the support, consultations, and incentive, and who allowed the independence to carry this thesis through to its final form. My committee members; John Baross, Bob Worrest, and John Baham, were all hepful beyond the call of duty, especially during the final crunch. Bob's critical consultations and assistance were especially valuable. And, not least, the technical and academic staff of the School of Oceanography are people I'm very happy to have worked with and come to know.

As much as I would like to, I don't think I can mention all the people who have made my stay here one of the best experiences of my life. Between canoe trips, Beanery trips, fluted and folksie musical experiences, parties, camping, tennis, movies, 23,742 dinners (for which someday I will repay you all), 'windsurfing', volleyball and saunas, psychoanalysis sessions, margueritas, the psychic experience of telemark skiing, and the wonderful friendship, it's a wonder that I had any time at all for a thesis. It is also a wonder that the time has come to leave it all (for the moment anyway) - something I have not looked forward to and tried not to think of. Fortunately, the end result is the knowledge that there are now many more people

who I can look forward to seeing again.

This work was supported by the Office of Naval Research, contract number N00014-79-C-0004, at the School of Oceanography, Oregon State University.

TABLE OF CONTENTS

LIST OF FIGURES

LIST OF TABLES

CHARACTERISTICS OF PHOTOCHEMICAL PRODUCTION OF CARBON MONOXIDE IN SEAWATER

I. INTRODUCTION

Dissolved carbon monoxide (CO) exhibits a dynamic distribution pattern within the marine euphotic zone which actively reflects the relative expression of physical, chemical, and biological processes that result in its production, consumption, vertical and horizontal transport, and exchange with the atmosphere. These processes are not well understood and are complicated by being spatially and temporally variable. Thus a priori predictions of chemical species distributions such as CO are difficult. However, an understanding of the chemical properties of carbon monoxide combined with knowledge of distribution patterns can help describe the presence and relative influences of factors which act on sources and sinks for CO.

Carbon monoxide occurs in surface ocean waters generally at concentrations much greater than would be predicted if a state of equilibrium with atmospheric CO existed. Its concentration also appears directly related to the intensity of global (sun + sky) radiation incident at the sea surface. High measured concentrations of CO have led several investigators to conclude that the oceans could be a significant source of CO to the atmosphere based on estimated rates of exchange at the air-sea interface (Linnenbom et al., 1973; Seiler, 1978).

Since CO is part of the marine carbon cycle, mechanisms by which it is produced and consumed will have a direct bearing on the origin

and fate of carbon compounds and other substrates. Alteration of organic compounds by processes that yield CO could result in production of transient compounds that are biologically more labile, other chemically reactive species, or more refractory organic matter. Microbial studies have demonstrated the existence of organisms which use CO as a source of energy and cell carbon (Meyer and Schlegel, 1979; Uffen, 1976), and soil communities that can consume CO when it occurs in concentrations above certain equilibrium values (Seiler, 1978; Conrad and Seiler, 1980b). Links have been made between CO and the metabolic cycles of other biologically important trace gases such as hydrogen, methane, and carbon dioxide (Ferenci, 1976; Seiler and Schmidt, 1976; Uffen, 1976; Hegeman, 1980; Higgins et al., 1980). Carbon monoxide is also capable of inhibiting specific metabolic functions such as nitrogen fixation and hydrogenase enzyme activity (Burris, 1979). It should be apparent from the preceeding points that CO can potentially play a significant role in marine microbial ecology.

Carbon monoxide production in surface waters is related to the incident light intensity, and recent studies suggest that CO may be the product of photochemical rather than strictly microbial processes (Wilson et al., 1970; Conrad and Seiler, 1980a) as has generally been proposed. At present, the field of marine photochemistry is poorly developed and few recorded studies of specific light induced processes and associated techniques are available. Sea water as a reaction medium is a diverse mixture of simple, complex, and largely unknown compounds in dissolved and particulate forms, and the subsurface light field is difficult to measure in a chemically

meaningful way. As a result, it is extremely difficult to bridge the gap between the complexity of the seawater medium, and knowledge gained from well defined laboratory experiments that use simple reaction media and classical photochemistry techniques. Yet the energy available as light quanta passing through the sea surface is sufficient in principle to induce almost any chemical reaction. Information concerning specific photo-induced reactions in seawater will contribute to a better understanding of the overall field of natural photochemistry.

The focus of this study was to determine characteristics of photochemical production of CO in seawater that relate to the quantity and quality of the incident light spectrum, dissolved oxygen concentrations, and potential precursor compounds. Additional tests were also made for biological versus abiotic production of CO. From this information, a potential mechanism for the photochemical production of CO is proposed. The results and conclusions help to point out areas and methods that should prove fruitful for further research.

Following is a summary of descriptive and experimental studies from the literature relating to CO in seawater. A brief summary of topics relevant to the experiments, interpretations of results, and discussion are included.

II. BACKGROUND

A. Marine Carbon Monoxide Distribution

Since 1968 dissolved carbon monoxide concentrations in surface waters and at depth have been measured at a variety of locations in the Pacific and Atlantic oceans (Swinnerton et al., 1969, 1970a,b, 1974, 1976; Lamontagne et al., 1971; Seiler and Junge, 1970; Seiler and Schmidt, 1974; Linnenbom et al., 1973; Conrad and Seiler, 1980a). Most of the data have been summarized by Seiler and Schmidt (1974) and Swinnerton et al. (1976), and several recurrent features indicate the action of specific processes that influence the distribution of CO.

Surface ocean waters (0 to 7 m) are nearly always found to be supersaturated in CO relative to the atmospheric partial pressures (or mixing ratios) of CO.[1] For typical marine atmospheric concent- rations between 0.1-0.2 ppmv the equilibrium concentrations range between 0.8-1.4 nM (18-31 nl l^{-1}).

Saturation ratios as high as 140 (actual concentration = 9.4 nM) have been recorded in the north Atlantic, and ratios between 5 and 30 are common. Undersaturation seems to occur infrequently, but has been recorded in surface waters at high latitudes of the north and south Atlantic (Seiler and Schmidt, 1974).

[1] The saturation ratio, R, is defined as the ratio of the actual or measured gas concentration in the liquid phase to the atmospheric equilibrium concentration under calm conditions that is predicted by Henry's Law: $R = C_{meas}/C_{equil}$. Saturation ratios greater than unity indicate supersaturation relative to the atmospheric partial pressure, and values less than unity indicate undersaturation.

Vertical profiles of dissolved CO also show recurrent patterns. Measurements by Swinnerton et al. (1968) in the Mediterranean, Linnenbom et al. (1973) in the North Atlantic, and Seiler and Schmidt (1974) in the Gulf of Cadiz reveal smooth gradients within the euphotic zone with highest CO concentrations usually occurring at or near the surface and decreasing to levels just over saturation below the euphotic zone (0.05-2.3 nM). Carbon monoxide concentrations in the remainder of the water column appears to be fairly constant (slightly supersaturated) except for higher concentrations found near the sediment-water interface (2.3 nM), and occasional high concentration anomalies at intermediate depths (Seiler, 1978). One such anomaly observed in the Gulf of Cadiz at 500 m (Seiler and Schmidt, 1974) could be explained by an influx of Mediteranean water. Other anomalies have not been acounted for as yet, and their regularity or duration are unknown. Early data collected by Seiler and Junge (1970) show maxima occurring at 100 m in the north Atlantic although no mention is made of protecting the samples from light (samples were collected and stored in glass bottles). As was later demonstrated, exposing water samples to light can result in increased CO (Wilson et al., 1970; Conrad and Seiler, 1980a; Bullister et al., 1981). This data must therefore be considered tentative. It should also be noted that early publications of dissolved CO concentrations in seawater did not always report the time of sample collection, weather conditions, or other factors related to light levels.

Based on the high surface concentrations of measured CO (and predicted), the oceans have been described as a source of CO to the atmosphere (Linnenbom et al., 1973; Seiler, 1978). However, the

magnitude of this source is still uncertain due to debatable assumptions used in calculations concerning the mechanisms that produce and consume CO, such as the rate of CO consumption relative to diffusion loss across the air-sea interface. In addition, despite the wide range of CO concentrations reported for surface waters, measured surface air concentrations generally remain constant at 0.1 to 0.3 ppm by volume (Seiler and Schmidt, 1974), though some correlation has been observed between surface water and atmospheric concentrations by Linnenbom and Swinnerton (1970).

The most notable feature of measured surface CO concentrations and near surface profiles are the diurnal fluctuations and apparent dependence on ambient light levels. Swinnerton et al. (1969, 1976), Lamontagne et al. (1971), Linnenbom et al. (1973), Seiler and Schmidt (1974), and Wilkniss et al. (1979) have documented the periodicity of CO concentrations at depths between 0.5-7 m at a number of locations. They have found CO to increase from slightly supersaturated levels at early morning hours to peak values at approximately 1400-1600 hr (local time) followed by a rapid decrease to original concentrations within 6 h as light levels decline. Concentrations can vary by factors of 2 to 20. Although CO concentrations in most of these studies have been plotted against time of day rather than actual measured light levels, light spectra, or other parameters such as light absorption characteristics of the water, there appears to be a delay in the maximum CO concentration relative to peak light levels. A recent study by Conrad and Seiler (1980a) which does relate measured visible light intensity to CO concentrations at a site in the Atlantic supports this observation. (In this case, peak light

intensity occurred at approximately 1300 hr and peak CO concentrations occurred at approximately 1600 hr.)

Changes in the vertical distribution of CO have also been measured and related to varying incident light levels by Linnenbom et al. (1973) and Seiler and Schmidt (1974). The resulting gradients show constant deep CO concentrations with more pronounced increases toward the surface when surface light intensities are high. At low light levels, the gradient can almost disappear.

Physical processes such as advective mixing, molecular diffusion, and gas exchange at the air-sea interface undoubtedly affect the CO distribution in seawater. For instance, turbulent mixing during storm conditions will enhance the exchange of dissolved gases with the atmosphere and result in either near-equilibrium concentrations, or supersaturated concentrations caused by bubble injection and dissolution.

However, since purely physical processes cannot account for the high CO levels found in surface water, and since a relationship between CO concentrations and light levels exists, other biological and/or chemical mechanisms must play an active role in its production and consumption. From their early studies, Swinnerton et al. (1970a, 1976), Seiler and Schmidt (1974), and Lamontagne et al. (1971) postulated a biological mechanism for the observed high concentrations of CO based on similar arguments. High concentrations of CO have been correlated to nutrient levels (Swinnerton et al., 1976; Sester et al., 1981), chlorophyll a (Conrad et al., 1982), and dissolved organic carbon (Lamontagne et al., 1970; Wilson et al., 1970). There is evidence, too,that specific organisms such as

certain algae, cyanobacteria, and siphonophores produce CO (Nozhevnikova and Yurganov, 1978).

Swinnerton et al. (1969) also noted the possibility that photochemical processes could play a role. Wilson et.al. (1970) demonstrated that CO production could be directly related to visible light and dissolved organic matter, by adding phytoplankton extract in varying concentrations to sterilized distilled water or seawater and exposing the solutions to fluorescent lights. They also reported that CO was produced, although in smaller amounts, in sterilized seawater samples that were kept dark.

More recently, Conrad and Seiler (1980a) have postulated that natural increases of CO in seawater are due to photo-oxidation of organic matter, and that the subsequent decrease of CO with the decline in light intensity is due to microbial consumption. These conclusions are based on experiments where seawater samples in glass containers were sterilized by poisoning with sodium azide or by 0.2 μm filtration and exposed to sunlight which resulted in CO production. Sterilized samples produced CO continuously, even for a period after the light was removed. This was explained as a delayed chemical reaction activated by exposure to light. Dissolved CO in unsterilized samples, or the other hand, demonstrated a diurnal cycle similar to that observed in ocean studies and included a production curve that lagged behind the light intensity curve. Earlier work by Seiler (1978) and others have shown that isolated bacteria and soil samples can consume CO.

Although not stated in their report, the initial rate of CO production (prior to 1200 hr) in the unsterilized samples was twice

the production rate of the azide poisoned samples while the filtered samples seemed to have a production rate similar to that in unfiltered samples (These phenomena will be addressed later, in the Discussion).

In another study, Hannan et al. (1980) irradiated algal cultures of Phaeodactylum tricornutum with varying fluxes of fluorescent UV radiation (290-400 nm) and visible light and concluded that UV-B radiation is not an agent for CO production in the algae cultures (the UV-B waveband is the portion of the solar ultraviolet spectrum that overlaps with the DNA absorption-"action" spectrum, 290-320 nm). The data that is reported however does not necessarily exclude the possibility that ultraviolet radiation significantly affected CO in the experiments.

B. An Overview of Marine Photochemistry Relative To CO Production

The solar spectrum: Solar radiation at the earth's surface ranges from the middle ultraviolet range (290-400 nm) to beyond the infrared (greater than 800 nm). The shorter wavelength range from 290-320 nm is greatly attenuated in the upper atmosphere primarily by absorption by ozone. This range (UV-B) is significant for its adverse affects on biological activity (Worrest et al., 1978, 1981a; Smith and Baker, 1982).

The energy equivalence of one Einstein (one mole of photons) at a specific wavelength is given by:

$$E = Nhc/\lambda = 1.197 \times 10^{5}/\lambda \text{ (kJ Einstein}^{-1}\text{)}$$

where N is Avagadro's number (6.023×10^{23} $mole^{-1}$), h is Planck's constant (6.63×10^{-37} kJ s), c is the speed of light (2.998×10^{17} nm s^{-1} in vacuo), and λ is the wavelength of light in nanometers. The solar ultraviolet and visible spectrum has an equivalent energy range of about 420-150 kJ $Einstein^{-1}$. Figure 1 (adapted from Zika ,1981) shows a typical spectral distribution in terms of wavelength and energy equivalent, along with some typical bond dissociation energies that are represented in marine organic matter. It would appear from an initial observation that the natural global light spectrum in the ultraviolet (290-400 nm) and blue (400-490 nm) regions have sufficient energy in principle to initiate most chemical reactions. The likelihood of a particular reaction, however, depends on whether the radiation is actually absorbed, the light intensity, concentrations and nature of photo active species, etc.

A typical, average light flux at the sea surface in the visible and ultraviolet regions is approximately 3.2×10^{25} photons m^{-2} h^{-1} (Zepp and Cline, 1977), and varies with latitude, time of day, weather, etc. Some loss occurs by reflection at the surface, and backscatter, however, approximately 90-95% of the radiation passes through the sea surface and is ultimately absorbed by water, dissolved species, or particulate matter. As an example of the significance of this flux, a typical increase in the concentration of CO by 36 nM (R = 30) in one cubic meter of seawater during one hour would require absorption of only about 2.2×10^{19} photons (0.000,000,7 of the average flux) assuming one photon results in one reaction.

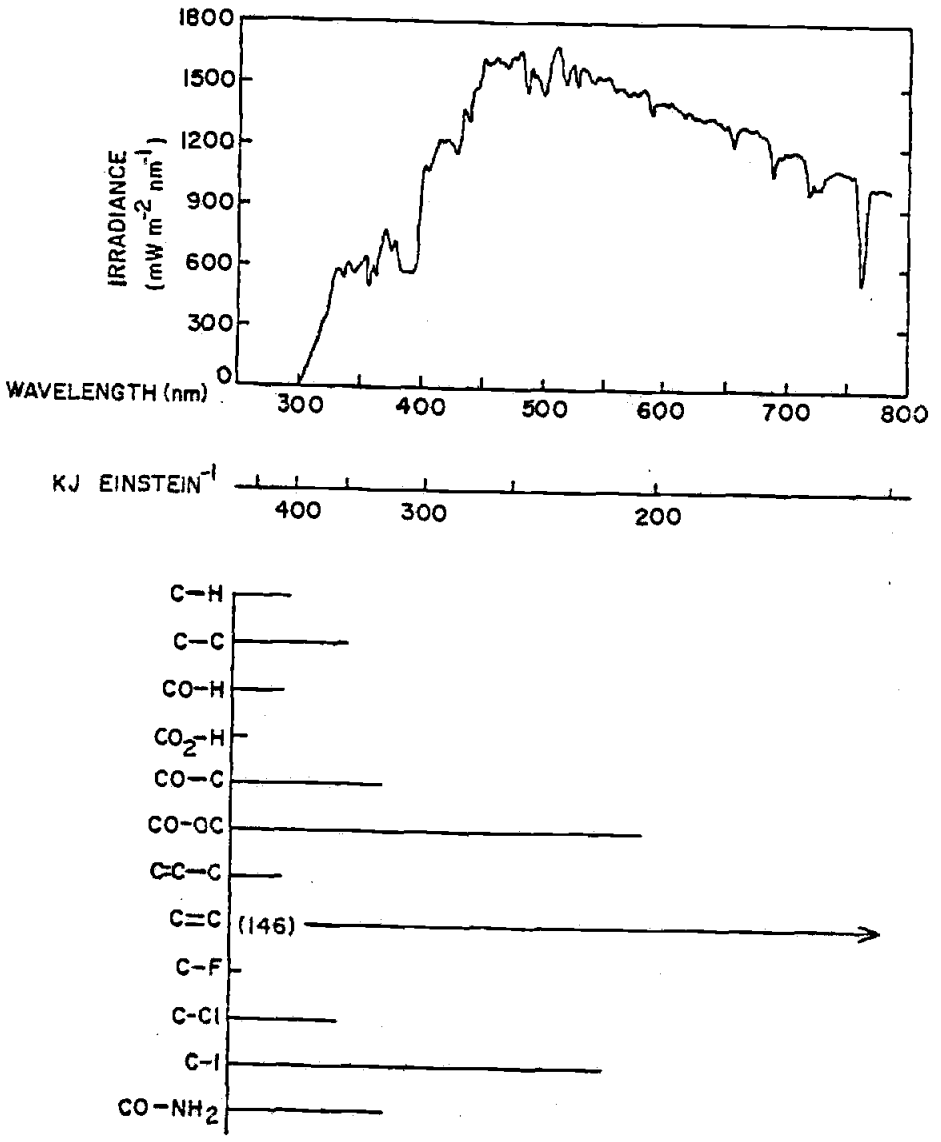

Fig. 1. Solar spectrum (recorded in Corvallis, Oregon during this study) and typical bond dissociation energies (adapted from Zika, 1981).

General marine photochemistry and photochemical processes:

Very little work has been done in the field of natural marine photochemistry, especially relative to marine organic matter. Little of classical photochemistry can be applied to the processes that take place in seawater because of fundamental differences between experimental designs and the aquatic environment. Organic solvents are usually employed in solution photochemistry since water significantly alters the electronic state of solutes. Oxygen, which is an efficient quencher and photoreactive species, is usually strictly excluded. Low temperatures are preferred to simplify the absorption spectra of a reactant, and to reduce reaction rates as well as the variety of products. Light sources emitting discrete lines or narrow wavebands at wavelengths that are shorter than those normally encountered in the solar spectrum are employed in contrast to the broadband polychromatic solar radiation at the earth's surface. Finally, simple systems with few, or single components in high concentrations, are desired, and reaction rates are on the scale of nanoseconds to hours. But in nature, significant reaction rates for many processes are of the order of days or years (e.g. turnover of refractory organic carbon).

The seawater matrix must be considered to be an extreme of unknown absorbing, sensitizing, and quenching species in low or highly variable concentrations with high concentrations of oxygen and particulates with large specific surface areas. Particulate matter may provide especially photo-reactive sites due to the concentration of metals, photosynthetic apparatus, and condensed organic matter. Nevertheless, fundamental properties of natural photochemical

processes can be studied and information can be gained that suggests possible reaction mechanisms and conditions.

A photochemical reaction involves absorption of a photon by a molecule or functional group (a chromophore), which results in the transfer of an electron to an excited, and less stable energy configuration (singlet or triplet). The basic law of photochemistry is that only absorbed light will result in excitation, and that 100% of the photon energy is absorbed (Raman scattering is one exception). The excited electronic configurations of organic chromophores usually fall into categories known as "singlet" or "triplet" states depending on the electron spin pairing. Triplet states, which can be achieved by a number of mechanisms (Horspool, 1976) are significant since return to the ground state is formally forbidden in a quantum mechanical sense, and therefore the lifetime (10^{-13} s) is sigificantly longer than the singlet state (10^{-15} s). This difference makes inter- and intra-molecular reactions more favorable.

Absorption of light is followed by reactions or transformations which can be considered either primary or secondary to the absorption process. Primary reactions can be redox reactions (charge transfer), bond cleavage and free radical formation, structural changes, transfer of energy to another species such as oxygen, or return to the ground state configuration. At the typical light flux and chromophore concentrations in seawater, most primary reactions are assumed to result from capture of a single photon. Therefore, the energy of absorbed light must be of a sufficiently short wavelength for a reaction to occur.

Secondary reactions are usually diffusion controlled processes

involving reactions of the primary products with other species. For example, partially oxidized groups may be primary products which are then susceptible to further (chemical or microbial) oxidation or modifications. Formation of free radicals, which initiate sequences of chain reactions ending only by combination of radical pairs, may be one of the most prevalent forms of organic alteration and auto-oxidation.

Although nearly all presently known natural dissolved organic compounds are transparent to radiation above 300 nm (Zafiriou, 1977), light absorption by organic matter does occur up to the 600 nm range. This is due primarily to particulate matter, pigments, and the remaining dissolved organic matter which, although uncharacterized, makes up approximately 90% of the total dissolved organic carbon. Exceptions to this are compounds such as vitamin B_{12} (Carlucci et al., 1965) which has one of the highest measured excitation rates, porphyrin compounds, ketones, and aldehydes which absorb appreciably in the UV and blue regions (UV Atlas, 1966). Inorganic constituents have only a minor influence on light absorption but contribute significantly to light scattering and therefore to the attenuation coefficient (absorption + scattering). Water, as a pure solvent, seems to be quite transparent to ultraviolet light (contrary to common misconception) (Zepp and Cline, 1977; Hannan et al., 1977). Although the absorption coefficient of water in the UV range is low in comparison to other dissolved constituents water may be the principal absorber of UV light due to its high relative concentration and the long light path lengths available.

A well known class of photochemical reactions involving carbonyl

containing compounds are known as "Norrish Type I" fragmentation reactions (Coxon and Halton, 1974; Horspool, 1976). The carbon-carbonyl bonds of ketones, $R-C(=O)-C-R$, are weak and concentration of vibrational energy at these sites from photoexcitation leads to cleavage and formation of a radical pair (Eq. 1). The bond dissociation energy for the carbon-carbonyl bond in acetone is approximately 335 kJ mol^{-1} which corresponds to UV radiation of about 360 nm.

Of a myriad of possible subsequent reaction pathways and product combinations involving free radicals (especially in seawater), one is cleavage of the second carbon-carbonyl bond resulting in formation of CO (Eq. 2). Alternatively, the carbonyl radical can abstract a hydrogen atom from another molecule resulting in the production of an aldehyde (Eq. 3). Aldehydes can also eliminate carbon monoxide by a similar scheme (Eq. 4).

$$R_3C-C(=O)-CR'_3 \longrightarrow R_3C-C(=O)\cdot + \cdot CR'_3 \qquad (1)$$

$$R_3C-C(=O)\cdot \longrightarrow R_3C\cdot + CO \qquad (2)$$

$$R_3C-C(=O)\cdot + HR \longrightarrow R_3C-CH(=O) + \cdot R \qquad (3)$$

$$R_3C-CH(=O) \longrightarrow R_3C\cdot + H\cdot \qquad (4)$$

Carbon monoxide in the upper atmosphere, for example, is formed in part by UV degradation of formaldehyde H_2CO (Ehhalt and Volz, 1976).

It must be recognized that in a typical water column the

intensity and spectral distribution of light is highly variable. The quantum efficiency of a photochemical reaction (0) is defined as the ratio of the number of molecules of a specific product formed from the reactants to the number of light quanta absorbed by the reactant species. Since absorption of light and therefore the efficiency of primary processes will be highly wavelength dependent, the steady state concentrations of various reactants available for secondary processes will vary with the light field. For a specific photochemical product the rate of production at different depths will not necessarily be a simple function of the average light intensity.

The subsurface light field: Optical properties of seawater have been reviewed by Jerlov (1976), Zaneveld (1975), Smith and Baker (1981), and others. Although the theory of light behavior in seawater is fairly advanced, necessary measurements for biological and chemical applications are not very extensive or easily performed. The most useful measured parameter for the purpose of photochemical studies (and to some extent photobiology) is the scalar irradiance, E_o, which is defined as the total flux of light in the form of energy or photons arriving at a point from all directions around the point. This can be further defined to include either the total spectrum or a specific wavelength. Knowledge of E_o combined with absorption characteristics of the water or of its individual components would be the most useful measure of the potential impact of light on a chemical species at a specific point in the water column. Of course, the scalar irradiance is a function of depth, time, weather, surface irradiance, and water type making predictive modeling difficult. E_o would also be the most useful parameter

for photobiological studies except in cases where organisms are preferentially oriented relative to the light field. In these cases the geometric structure of light becomes important.

Unfortunately, E_o is not easily measured and the closest measurable equivalent is the spherical irradiance, E_s, which is the light flux incident on (collected by) a spherical surface. E_s is ideally related (though not in practice) to E_o by $E_s = E_o/4$ as a result of a cosine correction for the geometry of the collecting surface relative to the incident light path (Jerlov, 1968). An alternative method is described by Zepp and Cline (1977) where scattering is ignored as a first approximation. The average light path lengths through a horizontal layer of water of a certain thickness are calculated using estimates of the average skylight, direct sunlight intensities, and angles of incidence at the sea surface. Using representative diffuse attenuation coefficients for various water types and absorption coefficients for known pollutants, the extent of photolysis of these pollutants could be determined.

In the case of CO, it is the product of a reaction rather than the reacting species that is known. At present it can only be stated that the subsurface light field in general is composed of spectral components that are of sufficient energy and intensity to produce photochemical reactions relative to CO within the water column.

Figure 2 is an example of the spectral distribution of light with increasing depth. Because of its attenuation characteristics, seawater acts as a crude monochromator transmitting predominantly near ultraviolet, blue, and green light. The dominant wavelength

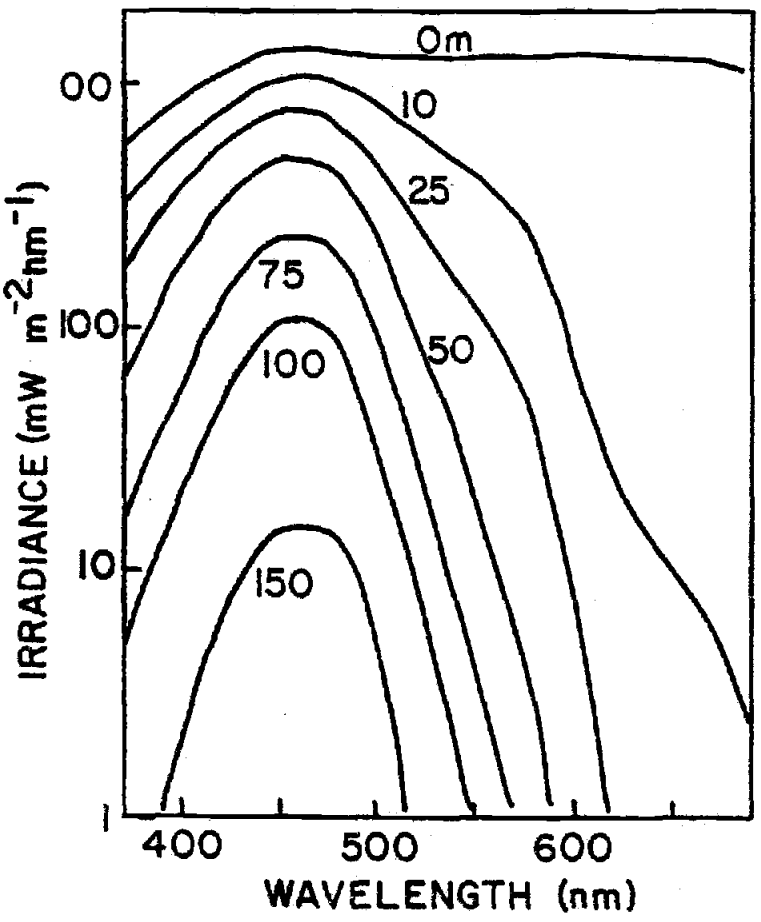

Fig. 2. Example of downwelling spectral irradiance recorded at various depths in clear ocean water of the Sargasso Sea (adapted from Lundgren and Hojerslev, 1971).

will depend on the composition and concentration of dissolved and particulate matter. High concentrations of dissolved organic matter, for example, will shift the spectrum to longer wavelengths. Figure 3 shows transmittance curves for different optical water types (higher numbers indicate greater DOM and particulate content). Figure 4 is a composite of collected diffuse attenuation data for relatively clear ocean waters.

Attenuation of light in a water column results from scattering and absorption of the light by various organic, inorganic, and particulate species present as well as water itself. Since absorption of light is the initial step in a photochemical transformation, it is interesting to note the absorption characteristics of seawater even if the actual chromophores are not known. Figure 5 is a typical absorption curve for "yellow substance" in seawater. Ultraviolet light is strongly absorbed while absorbance becomes minimal at longer wavelengths. The complex bonding structure and matrix of the organic matter is indicated by the lack of identifiable features in the absorption spectrum. Unfortunately, the spectral absorbance of light in seawater is not a commonly measured parameter. Nor is it easily separated from the apparent attenuation coefficient which includes scattering. Although this measurement could help to determine crude quantum yields for a specific reaction product species, its value is limited without further knowledge of the types of photochemical/photobiological transformations that occur and specific chromophores responsible for light absorption. It was pointed out that light in the blue region is selectively transmitted in seawater, but, lower attenuation in this region does not

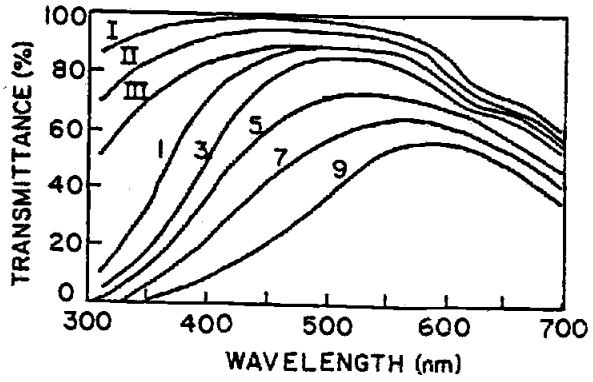

Fig. 3. Spectral transmittance (m^{-1}) for different water types. Increasing numbers indicate increasing organic and suspended content. I-III are oceanic and 1-9 are coastal waters (adapted from Jerlov, 1976).

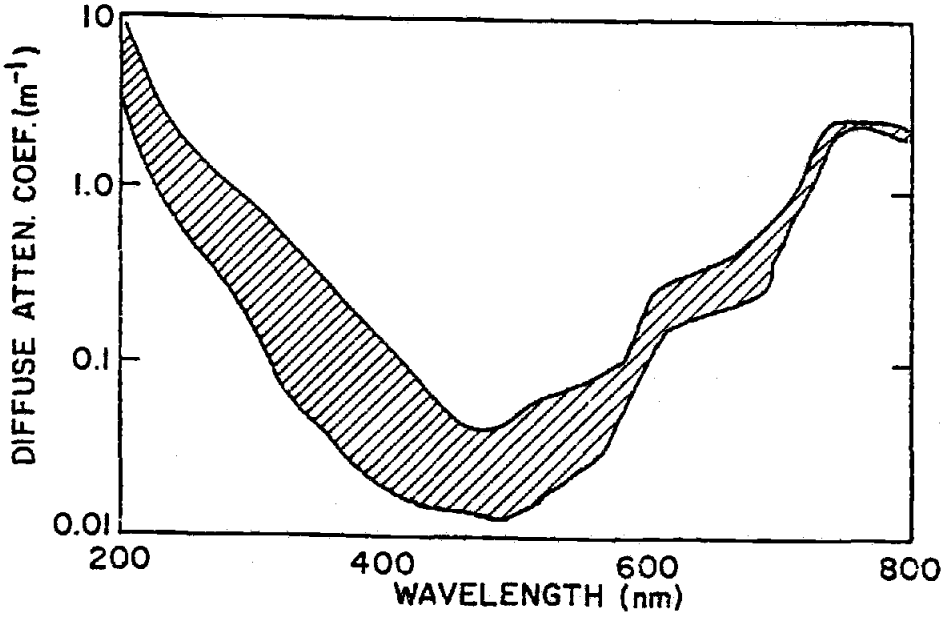

Fig. 4. Range of cumulative diffuse attenuation coefficients vs wavelength for ocean water (adapted from Smith and Baker, 1981).

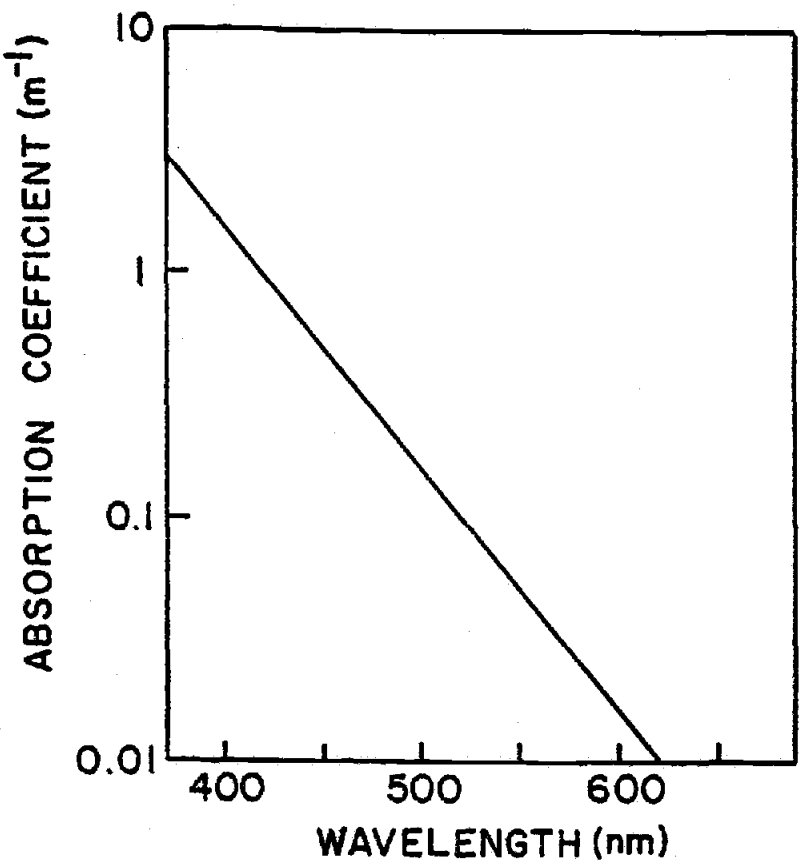

Fig. 5. Typical absorption curve for marine 'yellow substance' (Gelbstoff) (from Zaneveld, 1975).

necessarily mean reduced photochemical potential. Absorbing species may be in vanishingly small steady state concentrations if they are produced continually (e.g. biologically) and yet have extremely high reaction efficiencies. Their contribution to the overall light attenuation or absorbance could be minimal.

C. Biological Regulation of CO

Some of the biologic sources and sinks for CO are briefly described here. A more complete summary is given by Nozhevnikova and Yurganov (1978) and Junge et al. (1972). A number of macrophytic and unicellular algae are known to produce carbon monoxide. The brown algae Nereocystis lutkeana have flotation appendages, pneumatyocysts, that contain 5-12% CO by volume (Foreman, 1976), although it is not yet clear whether escape of CO from the algae to the water can be considered significant.

Siphonophores (Coelenterates) have gas filled floats, pneumatophores, which contain 90% CO (Pickwell, 1970). Specialized cells of the pneumatophores produce the CO from L-serine. Siphonophores have diurnal, vertical migration patterns during which CO is actively produced and released for buoyancy adjustment. Their distribution in the oceans is not well known since intact collection is difficult, however, it is possible that they are widespread. Bubbles made up predominantly of CO released at depth could greatly enrich the surrounding water in CO due to high hydrostatic pressures. Some of the deep anomolies mentioned earlier correspond to depths at which siphonophores have been found, and could conceivably be associated

with these organisms.

On a microbial level, CO has been observed to be formed by red algae and cyanobacteria through the breakdown of heme compounds (Nozhevnikova and Yurganov, 1978). Other marine bacteria (Alginomonas, Brevibacterium), yeasts, and "anaerobic microbial communities" have also been found to evolve CO although the mechansim is unknown. Bauer et al. (1980) claim that CO evolved from cultures of phototrophic organisms is caused by oxidative tissue breakdown and not by metabolic activity. The CO profiles observed immediately above sediment surfaces suggest (though do not prove) that CO is produced by sedimentary microbial communities.

Microbial consumption of CO is better documented than production. Marine organisms including green algae (Chappelle, 1962) and Desulfovibrio desulfuricans (Yagi, 1962), soil communities (Seiler and Schmidt, 1974), carboxydobacteria, and methane oxidizing bacteria (Ferenci et al., 1975; Ferenci, 1976) are known to consume CO. Only carboxydobacteria are known to be able to use CO as the sole source of energy and cell carbon, although other substrates such as H_2 and CO_2 are preferred (Zavarazin and Nozhevnikova, 1977). Common features of CO consumption are: 1) Uptake is usually non-specific, 2) other substrates are usually preferred, and 3) no unique metabolic pathway seems to exist for the utilization of CO although several hypothetical pathways have favorable energy yields. It is known, however, that in some cases CO is utilized as CO_2 by a preliminary oxidation step.

D. Dissolved Gases

The equilibrium concentration of an inert dissolved gas at dilute concentrations is expressed by Henry's Law:

$$C_{equil} = a(T,S) \times p \qquad (5)$$

Using units that are consistent with other published data, C_{equil} is the gas concentration in (ml of gas at STP) (ml of water)$^{-1}$, p is the partial pressure (atm) of the gas in the gas phase over the liquid, and the Bunsen solubility coefficient a(T,S) is the volume (ml) of gas at STP (0 C, 1 atm) that is dissolved in one ml of liquid at equilibrium with the gas at one atmosphere (760 mm Hg) of pressure. The coefficient is a function of temperature and salinity and has units of (ml gas) (ml liquid)$^{-1}$ atm^{-1}. When actual gas concen- trations are greater than the predicted equilbrium concentrations (relative to the atmospheric concentration or partial pressure) the saturation ratio, R, is greater than unity, and the solution is said to be supersaturated. Conversely, a saturation ratio less than unity indicates undersaturation. The saturation ratio is useful for indicating nonequilibrium conditions, where production-consumption processes are taking place at rates greater than can be compensated for by exchange across the air-sea interface. As noted, high saturation ratios generally found in surface ocean waters have led to the conclusion that the oceans must be a net source of CO to the atmosphere.

III. GOALS

That carbon monoxide can be produced photochemically in seawater is consistent with the potential for organic photochemical reactions, the nature of dissolved organic matter, the subsurface light field, and experiments by Wilson et al. (1970), and Conrad (1980a) that suggest abiotic light induced CO production. Operating partly on this premise, the goals of this project were to determine some of the general photochemical characteristics of CO production. These would provide information on possible source mechanisms as well as data on the effect of light on substrate compounds and the nature of photochemical processes. Characteristics of carbon monoxide production to be tested were:

1) The relation between wavelength and efficiency of CO production.
2) The effect of dissolved oxygen concentration.
3) A test of CO evolved from a few organic compounds that may be considered representative of a broader class of functional groups likely to be found in the organic matrix of seawater.

IV. MATERIALS AND METHODS

Seawater samples were collected at various times throughout the study from the shore or from a boat at a point 1.2 km inside the south jetty of Yaquina Bay, Oregon. Samples were always taken within 20 minutes of high tide to obtain predominantly coastal ocean water and the salinity was measured using an Autosal Model 8400 salinometer. Bottles were thoroughly rinsed with sea water prior to filling and a polypropylene bucket was used to fill the bottles. The water received no special treatment except to avoid prolonged contact with rubber or plastic. Immediately after filling, the bottles were loosely capped with aluminum foil and covered to exclude light. Except when removing aliquants for experiments the samples were kept covered and stored at approximately 10 C. Generally, samples were used for experiments within three days of collection. Unless it is otherwise specified, samples were air-equilibrated.

Distilled water was prepared by redistilling house distilled water in an all glass still (Bellco). This water was not entirely free of substances that could produce carbon monoxide when exposed to light, but the levels of CO produced were low and could be subtracted as background.

Sodium azide (Practical), mercuric chloride, acetone("Photrex"), acetic acid ("Photrex"), hydrochloric acid (Reagent gr.), sodium hydroxide (Reagent gr.), sodium bisulfite (Reagent gr.) (all Baker), humic acid (Tech. gr., Aldrich), dextrose (Reagent gr., MCB), and acetaldehyde (Aldrich) were used without further purification.

Sample flasks for irradiating water samples were made of 30 mm

I.D. x 33 mm O.D. clear fused quartz tubing from Quartz Scientific Inc. ("SD-P", water free). The reported spectral transmission curve is shown in Figure 6. Each flask was 24 cm. long fitted with a quartz standard taper joint at one end and sealed at the other. Stoppers were Pyrex(R) with Teflon(R) sleeves. The volume of each flask was approximately 155 ml. when stoppered.

Quartz flasks and other glassware were cleaned prior to each experiment with a laboratory detergent ("Micro", Cole-Parmer), distilled water, acetone, distilled water, hot dichromate/H_2SO_4 solution, and then thoroughly rinsed with redistilled water. A final rinse was always done with the solution or sample to be put in the flasks. This procedure was found to be sufficient for cleaning relative to CO production. To fill the flasks, samples were simply poured in smoothly and the flasks were stoppered so that bubbles were not injected or trapped. When filled sequentially in this manner a set of samples with uniform concentrations of CO, H_2, CH_4, O_2 + Ar, and N_2 could be obtained.

In some cases samples were purged with gas (N_2, O_2, or air) prior to being transfered to quartz tubes. This was done by bubbling gas through the sample at 5 cc s^{-1} in a filter flask using a gas dispersion tube (Figure 7). The vent could then be closed and the sample would be forced through a glass siphon to the bottom of a quartz flask. When the sample was overflowing, the siphon tube would be slowly withdrawn, and the flask would be stoppered without trapping bubbles. Gases used were high purity N_2 with an Oxisorb(R) trap in line to remove trace O_2,

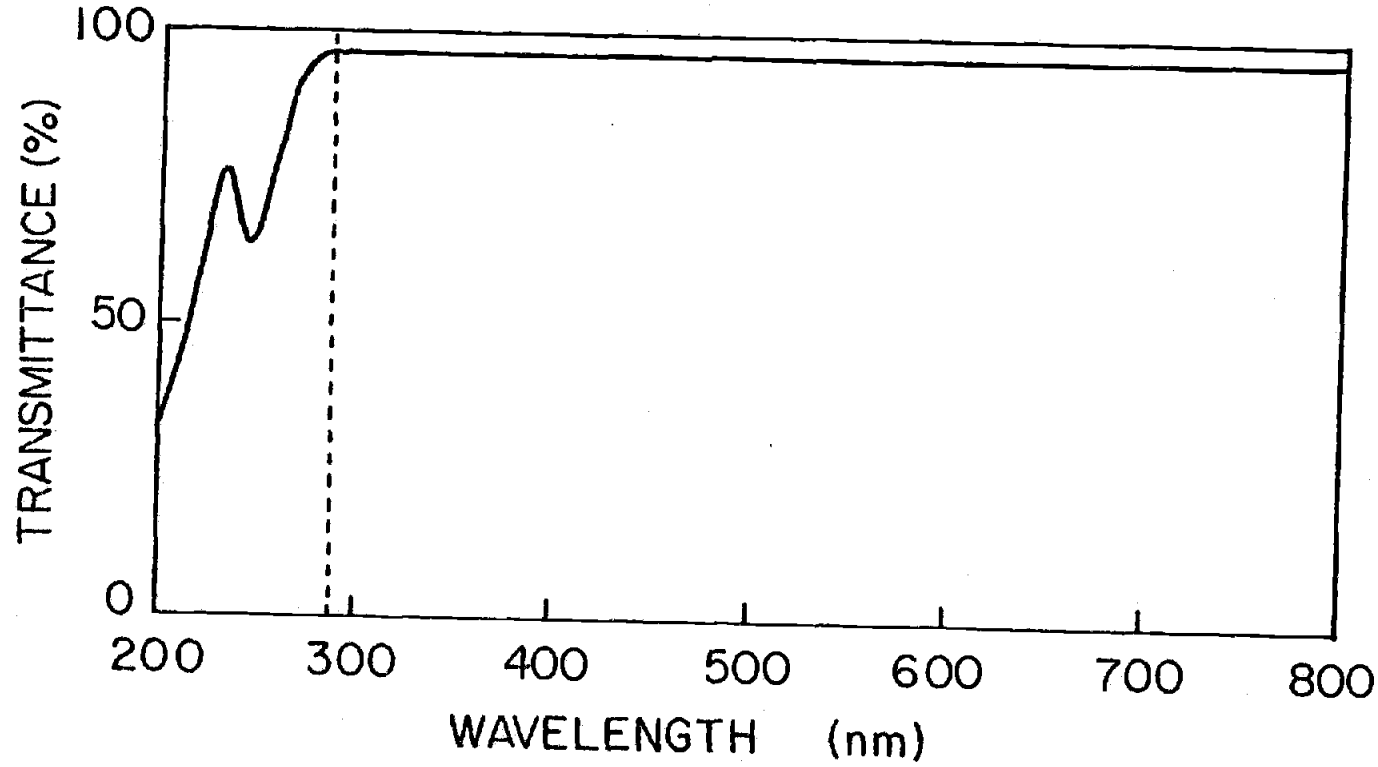

Fig. 6. Transmission curve of "SP-D" fuzed quartz (from Quartz Scientific Inc.).

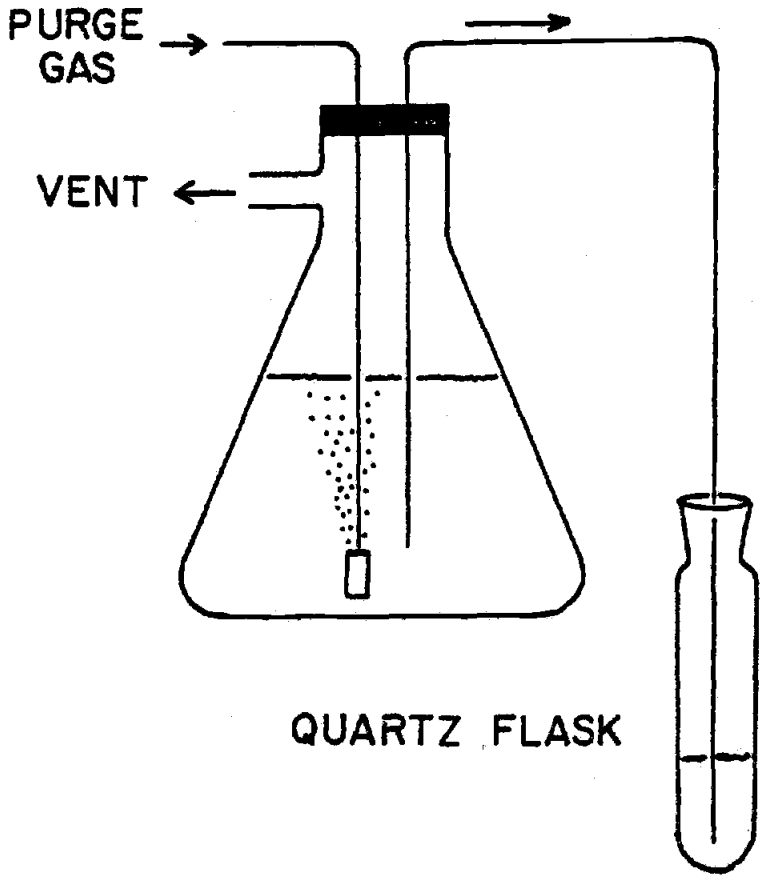

Fig. 7. Apparatus for purging water samples and transferring to quartz flasks.

extra dry O_2, or dry grade compressed air (Polar Cryogenics).

For autoclaving, samples and all associated glassware were heated to 250 C for 20 min. followed by a 1 h cool down period. One procedure was to autoclave samples in the quartz flasks capped with aluminum foil. The other procedure involved bubbling nitrogen through a sample in a 4 l flask to reduce the oxygen concentration, capping "tightly" with foil and autoclaving the sample, quartz tubes, and transfer glassware. After cooling, the samples would be transfered to the quartz flasks as quickly as possible while avoiding contamination. The flasks with samples would be cooled to 15 C in a water bath.

To expose samples to sunlight, filled quartz flasks were put in open faced boxes that were 10 cm x 36 cm x 6.5 cm (ht.) and painted black. Flasks were supported 1.5 cm above the base (Fig 8). The boxes were used to assure that each flask was exposed to an identical portion of the sky during an exposure period. The temperature of the flasks during an experiment was not controlled except a 1.3 cm gap between a filter and the top of a box allowed some cooling by convection. The samples did not experience temperatures above 31 C.

The apparatus for exposing samples to fluorescent light was a rotating table inside a black enclosure to exclude room light (Fig. 9). A 4 foot fluorescent light fixture with two lamps was mounted 24 cm above the center of the table. By mounting the flasks radially each sample would receive equal exposure. Filters could be wrapped around the flasks or mounted on a flat horizontal frame 10 cm beneath the lamps. A fan was used to circulate air and keep the temperature from rising above 26 C while the lights were on.

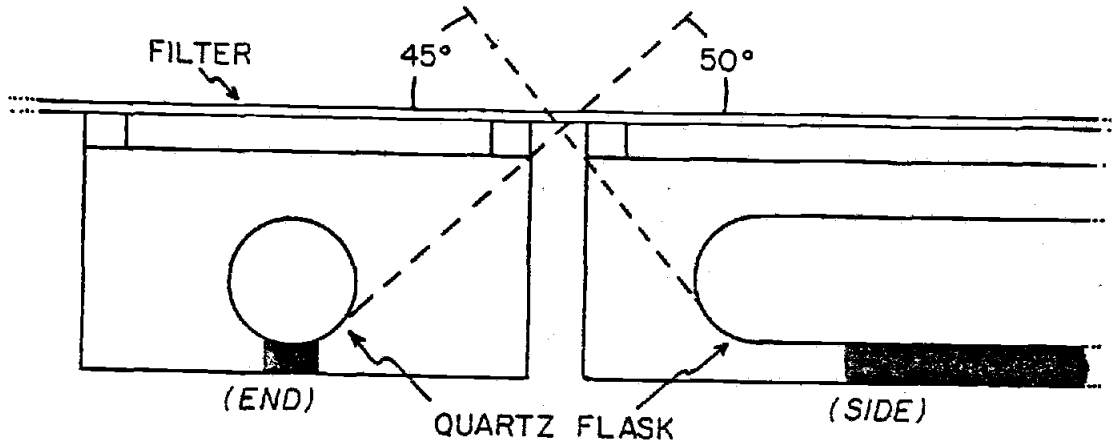

Fig. 8. Schematic of boxes used for exposing water samples in quartz flasks to sunlight. (Boxes were aligned such that no part of the flasks were in shadow).

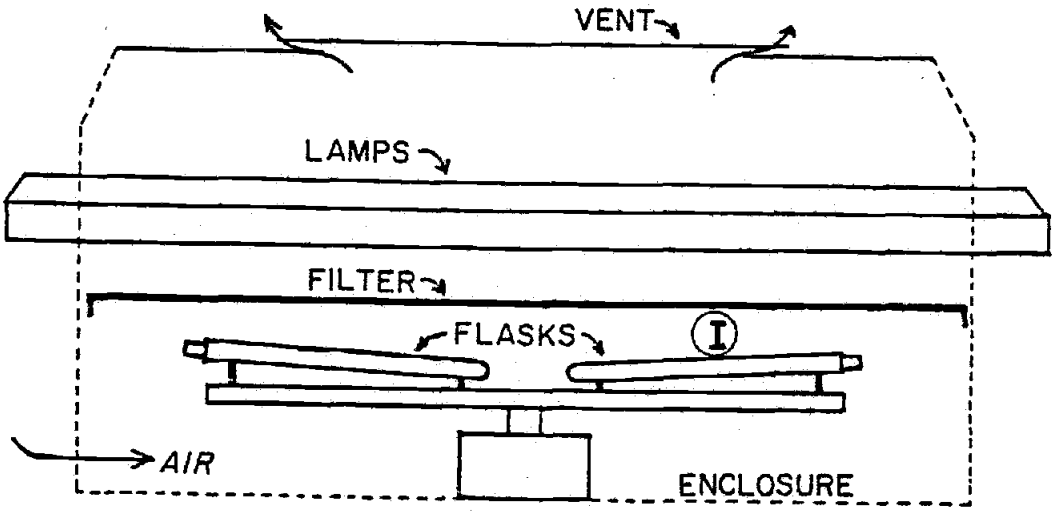

Fig. 9. Apparatus (with rotating table) used for exposing water samples to fluorescent lights.

Light sources were fluorescent lights, and sun + skylight. Experiments done using sun + skylight were done at solar elevations of 40 degrees or greater, and on clear or nearly clear days (i.e. no more than slight uniform haze). Fluorescent lights used were General Electric F40 and FS40, and Westinghouse F40BL (cool white, sunlamp, and blacklight respectively) and were aged 72 h before being used. Point "I" in Figure 10 indicates the position of a spectroradiometer collector head where spectral curves were measured, and is the position of the center of a quartz flask on the rotating table when it is parallel to the fluorescent light tubes. It is important to note that the spectral curves represent relative light spectra incident on the quartz flasks and not the actual integrated light intensity to which a sample was exposed.

Spectral filters used were 0.25 mm clear cellulose acetate, 0.18 mm Mylar "D", 3.2 mm clear polycarbonate, and 3.2 mm yellow acrylic plastic (Plexiglas$^{(R)}$, Rohm and Haas no. 2208) which have wavelength cutoffs below 290 nm, 315 nm, 400 nm, and approximately 500 nm respectively. Mylar and acetate filters were exposed to sunlight for 8 h and FS40 lamps for 24 h prior to use since the spectral characteristics are known to change rapidly during initial exposures (Worrest, 1981b).

Spectral data were obtained using an Optronic Laboratories Spectroradiometer Model 742 with ultraviolet and visible cosine collector heads. Irradiance was measured at 1 nm intervals from 250 to 360 nm, and at 2 nm intervals from 362 to 800 nm. A Hewlett-Packard 9815A Data Acquisition System was programmed to integrate spectral curves using Simpson's Rule (parabolic

approximation). Separate programs were written to convert irradiance to photon flux and integrate the generated curves.

Additional monitoring of light intensities was done using a Li-Cor Model LI-185A Light Meter with a cosine quantum collector head (Li-Cor Model Li-190S). The spectral response of the light meter is fairly constant in the 400 to 700 nm wavelength range.

Analysis of the dissolved gases in the sample tubes (CO, CH_4, H_2, O_2 + Ar, and N_2) was done by stripping the sample with a helium bubble stream, trapping the stripped gases on Molecular Seive 5A$^{(R)}$ cooled with liquid nitrogen, and subsequently analysing the gases by gas chromatography. A detailed description of the analysis procedure and calculations is provided in the Appendix.

V. EXPERIMENTS AND RESULTS

A. Light Dependent Production of Carbon Monoxide

Air saturated sea water samples in quartz flasks were exposed to sunlight to verify light dependent production of carbon monoxide, and to determine characteristics of the production for subsequent experiments. (Hereafter, "sunlight" will be used to refer to global radiation which is the sum of direct sunlight and diffuse skylight.)

One set of 11 samples was exposed to sunlight, and individual samples were removed after 1, 2, 3.5, and 5 hours for CO analysis. Light intensity measurements were recorded concurrently using a quantum meter (photons m^{-2} s^{-1}) at 30 min intervals during the experiment. The natural visible spectrum at the earth's surface is essentially constant for solar zenith angles less than 75 degrees (Jerlov, 1976). The shape of the ultraviolet spectrum greater than 310 nm also appears to be constant for solar zenith angles less than 60 degrees. (Baker et al., 1980). Since the zenith angle during this experiment (and all subsequent experiments) was always less than 60 degrees, the quantum measurements should be closely related to the irradiance over the entire spectrum except for variations in the 290-310 nm range (see Materials and Methods). Integration of the measured irradiance over time provides a measure of the total amount of light that has passed through a unit area, which in turn is related to the total light incident on the samples. Since the quartz flasks were tubular and were horizontally pointed toward the average position of the sun, it is assumed that the spectrum inside the

flasks was not significantly altered over time by surface reflection losses.

The quantum irradiance measurements, while related to the light intensity, is not the actual light flux, or distribution, experienced by the water samples. Reflection at the quartz flask surfaces reduces the light flux by approximately 10%. Also, the quantum meter has a spectral response between 400 and 700 nm which would not include the ultraviolet range (290 to 400 nm).

The quantum irradiance curve generated by periodic quantum meter readings was integrated by parabolic approximation (Simpson's Rule) (Fig 10). Measured concentrations of CO were then plotted against the integrated quantum irradiance (photons m^{-2}). The result was the linear relationship shown in Figure 11.

After the exposure period, the remaining flasks were covered and analyzed at one hour intervals for four hours to monitor changes in the CO concentrations. In two additional experiments, sets of flasks were exposed for two hours to: 1) sunlight, and 2) sunlight filtered through polycarbonate to eliminate most ultraviolet light. Some samples were also put in the exposure apparatus but covered with aluminum foil. These were then removed from the light and analysed for changes in CO at intervals during six hour periods. The results are plotted in Figure 12.

In all cases, the CO concentration did not vary significantly for the 4 h following exposure. These results indicated that in subsequent experiments, samples could be removed from the light and analyzed within a few hours without the CO concentration changing. Note that in each case, CO is highly supersaturated relative to the

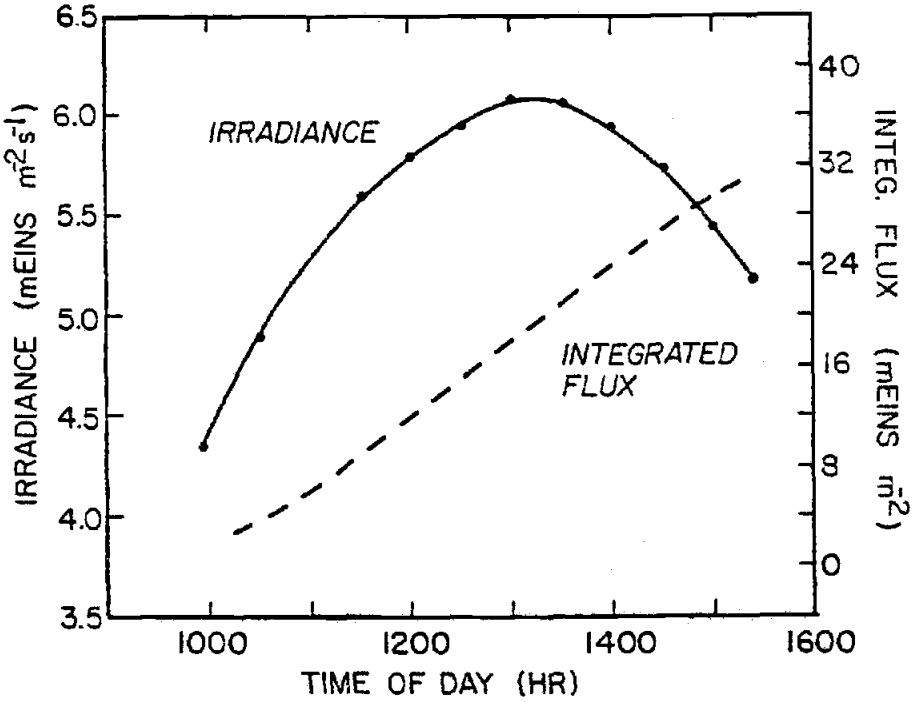

Fig. 10. Quantum irradiance vs time of day, and total irradiance (flux) integrated over time.

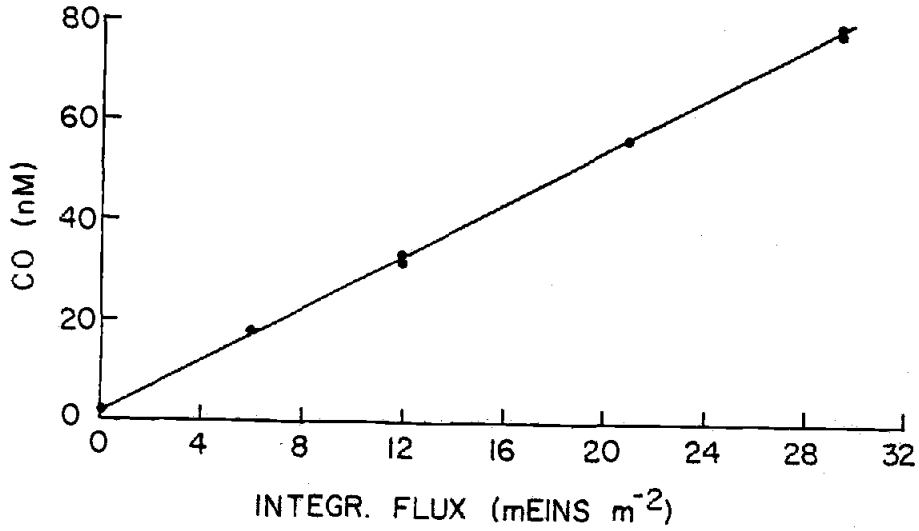

Fig. 11. Production of CO vs total irradiance (flux).

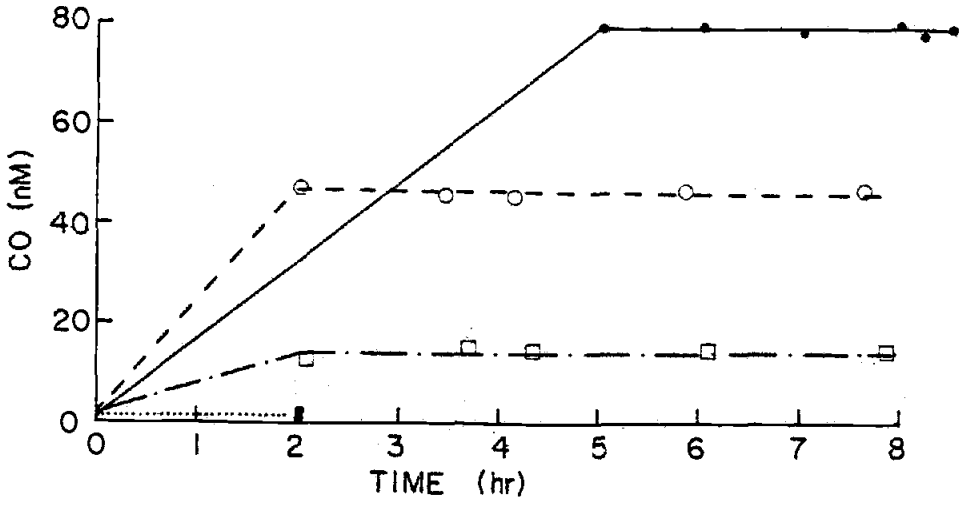

Fig. 12. Carbon monoxide concentrations in seawater samples following exposure to sunlight. Closed and open circles are samples exposed to unfiltered sunlight. Open boxes are samples exposed to sunlight filtered through polycarbonate. Dotted line are foil covered samples.

atmospheric equilibrium concentration of about 1 nM by as much as a factor of 800 (Equilibrium values were determined using data from Wiesenburg and Guinasso (1979)). This indicates that the flasks were not losing CO by diffusion during this time period.

B. Spectral Response of Carbon Monoxide Production

Seawater samples in quartz flasks were exposed to direct sunlight, and sunlight filtered through cellulose acetate, mylar, polycarbonate, and yellow acrylic plastic filters to determine the relative effects of different portions of the global spectrum (sunlight + skylight) on carbon monoxide production. Spectra recorded on a clear day at solar noon using these filters are shown relative to unfiltered sunlight in Figures 13 and 14. The general shapes of these spectra were assumed to be constant for all exposure experiments which were done on clear days. Cellulose acetate normally cuts off at 290 nm. However, since wavelengths less than this are not significant in the terrestrial solar spectrum, the effect of cellulose acetate is to attenuate the 290 nm to 360 nm portion of the spectrum with greater attenuation occurring at the shorter wavelengths. Mylar also attenuates light in this region, and, in addition it cuts off all light less than 315 nm. Polycarbonate absorbs nearly all ultraviolet light (less than 385 nm) and yellow acrylic plasic absorbs light less than about 465 nm (shortwave blue light). Reduction of light at longer wavelengths in each of these spectra is due primarily to reflection at the filter surfaces. This reduction is approximately 10% for the UV and visible

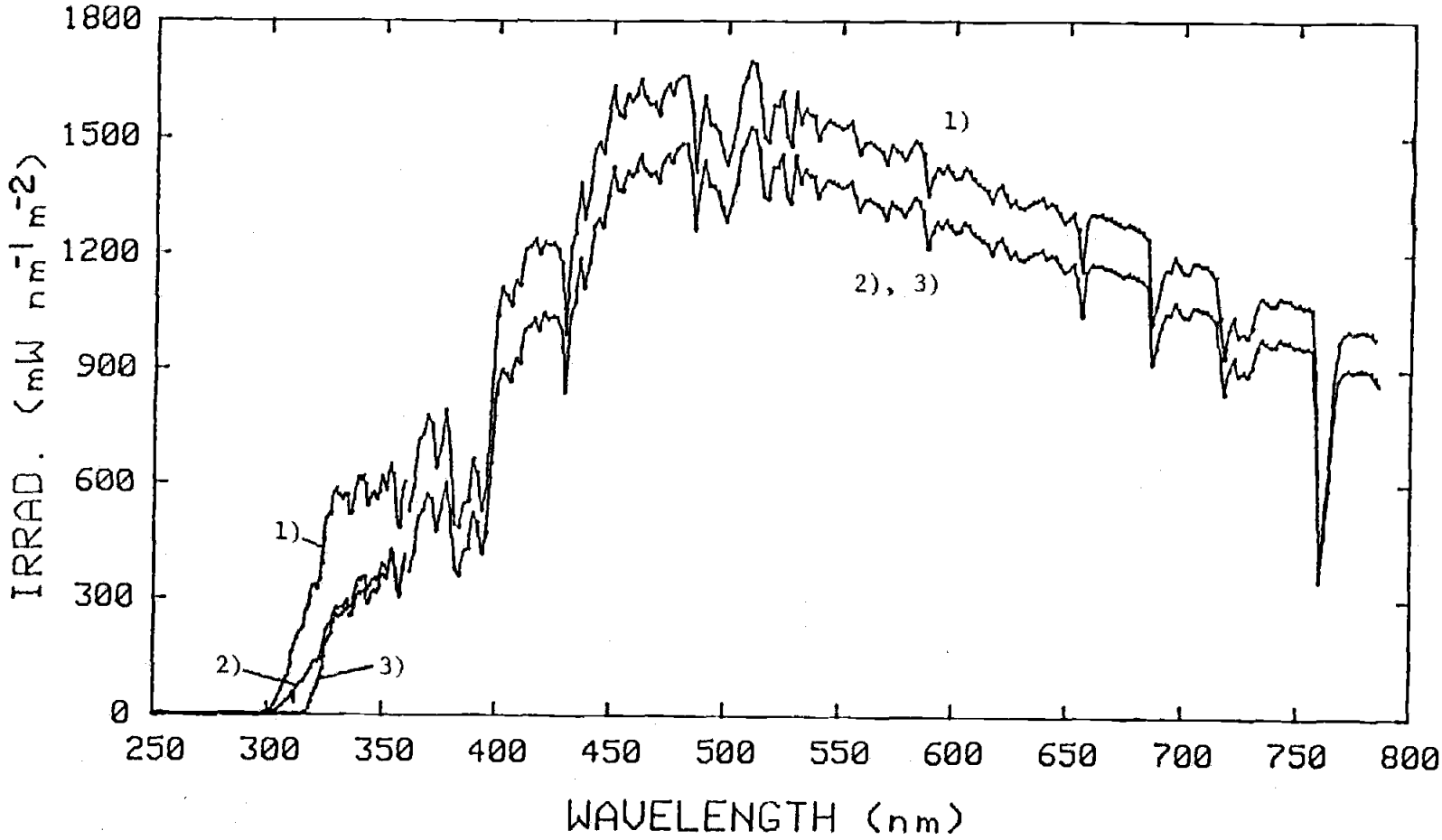

Fig. 13. Solar spectrum recorded in Corvallis, Oregon, on a clear day (1400 hr, June 12, 1982): 1) unfiltered, 2) filtered through cellulose acetate, and 3) filtered through Mylar.

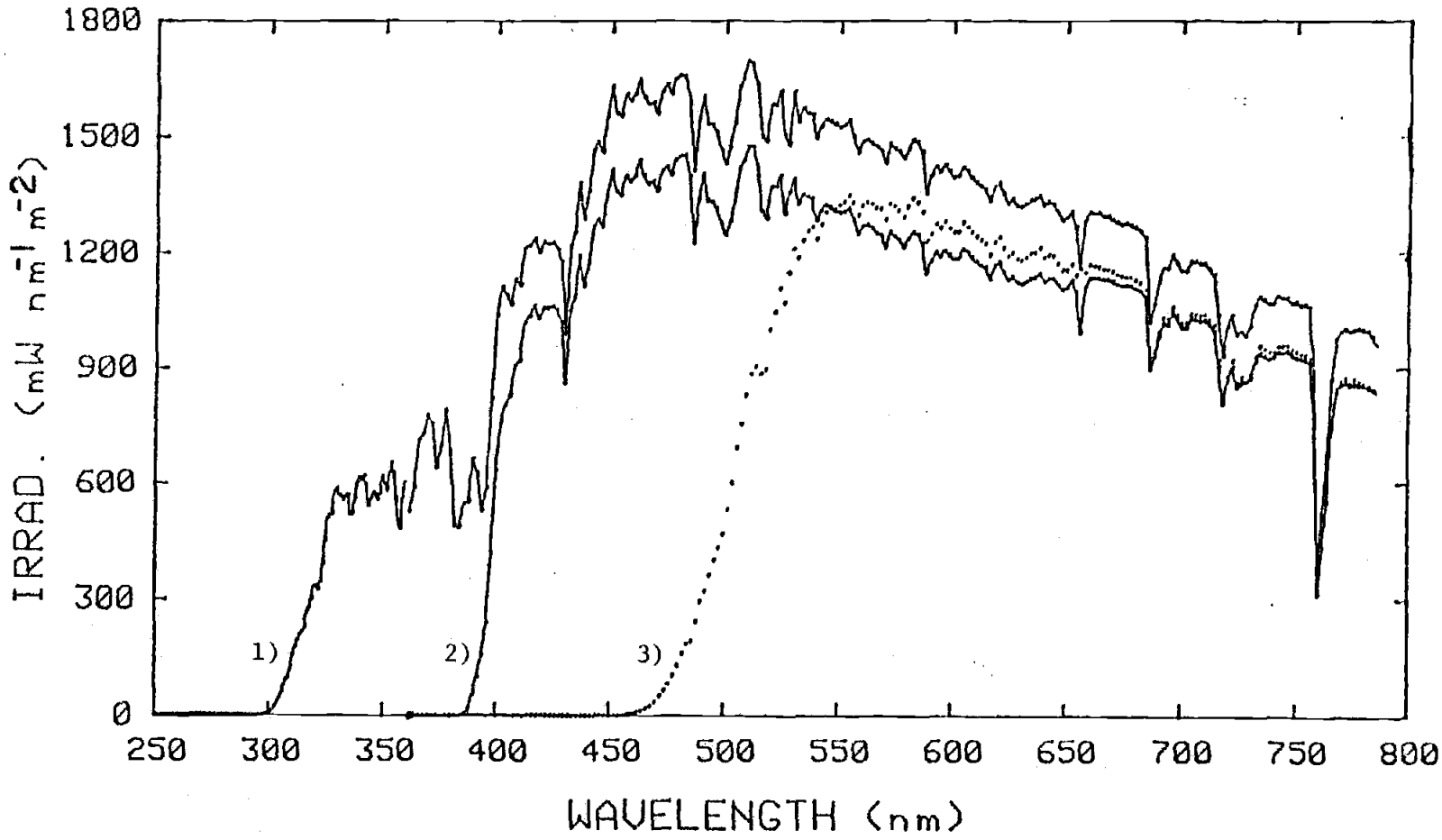

Fig. 14. Solar spectrum recorded in Corvallis, Oregon, on a clear day (June 12, 1982, 1330 hr): 1) unfiltered, 2) filtered through polycarbonate, and 3) filtered through yellow acrylic plastic.

spectrum. The effect of the quartz flasks on spectral transmission was to reduce the intensity of the entire spectrum by an additional 10% without significantly altering the shape of the spectrum.

Two sets of exposures were done on different days to test the range of spectra described. Seawater in each case was collected on different days but under the same conditions. Salinities were measured at 31.8 ppt for the first sample and 32.0 ppt for the second which is typical for Oregon coastal ocean water.

Each set of exposures involved exposing one group of seawater samples to light filtered through mylar and acetate, and a second group to light filtered through polycarbonate and yellow acrylic. Three flasks in each group were exposed to unfiltered sunlight. The other irradiated samples were then normalized to these samples to compensate for variations in the light intensity during and between sample sets. Also, two flasks in each sample set were covered with aluminum foil so changes in CO concentrations not directly related to light could be observed. Initial CO concentrations in the bulk water samples were measured immediately prior to filling the quartz flasks of each set of exposures.

Results of these experiments are listed in Tables 1 through 4. To compensate for attenuation by reflection from the filter surfaces, averaged CO production was increased by 10% for better comparison with samples exposed to unfiltered sunlight. The ultraviolet region is most effective in producing carbon monoxide, but light extending at least up to the blue region, (450-500 nm), also produce CO. Between 70 and 80% of the CO produced can be accounted for by exposure to light in the ultraviolet region.

Table 1. CO production in seawater sample set #1 exposed to sunlight using cellulose acetate and Mylar filters.

exposure period: 2 h
initial irrad. : 5200 uEinsteins m^{-2} s^{-1}
final irrad. : 3900 uEinsteins m^{-2} s^{-1}

flask #	filter	CO (nM)	CO_{avg} (nM)	dCO (nM)	CO_{norm}
initial	---	1.0		----	----
initial	---	1.5	1.3	----	----
1	n.f.	35.1			
2	n.f.	40.9	38.4	37.1	1.00
3	n.f.	39.1			
4	acetate	28.3			
5	acetate	29.9	<32.9>	31.6	0.85
6	acetate	31.5			
7	mylar	23.6			
8	mylar	24.8	<26.6>	25.3	0.68
9	mylar	24.3			
10	dark	2.1			
11	dark	2.7	2.4	1.1	----

n.f. = no filter (direct sun exposure)
CO_{avg} = average CO conc. for samples with the same filter

$dCO = (CO_{avg})-(CO_{dark})$

$CO_{norm} = (dCO)/(dCO_{n.f.})$

<> indicates values have been increased 10% to compensate for reflection at filter surfaces

Table 2. CO production in seawater sample set #1 exposed to sunlight using polycarbonate and yellow acrylic filters.

exposure period: 2 h
initial irrad. : 3400 uEinsteins m^{-2} s^{-1}
final irrad. : 5300 uEinsteins m^{-2} s^{-1}

flask #	filter	CO (nM)	CO_{avg} (nM)	dCO (nM)	CO_{norm}
initial	---	1.2			
initial	---	1.3	1.3	----	----
1	n.f.	31.6			
2	n.f.	31.5	31.9	30.6	1.00
3	n.f.	32.5			
4	polybarb.	7.2			
5	polycarb.	7.4	<8.1>	6.8	0.22
6	polycarb.	7.4			
7	y. plex.	3.3			
8	y. plex.	3.5	<3.9>	2.6	0.08
9	y. plex.	3.5			
10	dark	1.4			
11	dark	2.3	1.9	0.6	----

Tabel 3. CO production in seawater samples set #2 exposed to sunlight using cellulose acetate and Mylar filters.

exposure period: 2 h
initial irrad. : 4500 uEinstein m^{-2} s^{-1}
final irrad. : 5720 uEinstein m^{-2} s^{-1}

flask #	filter	CO (nM)	CO_{avg} (nM)	dCO (nM)	CO_{norm}
initial	---	0.5			
initial	---	0.5	0.5	-----	----
initial	---	0.6			
1	n.f.	19.8			
2	n.f.	20.4	19.9	19.4	1.00
3	n.f.	19.5			
4	acetate	16.9			
5	acetate	15.9	<17.7>	17.2	0.89
6	acetate	15.4			
7	mylar	13.6			
8	mylar	14.4	<15.3>	14.8	0.76
9	mylar	13.8			
10	dark	0.5			
11	dark	0.5	0.5	0.0	----

Table 4. CO production in seawater sample set #2 exposed to sunlight using polycarbonate and yellow acrylic filters.

exposure period: 2 h
initial irrad. : 5500 uEinstein m^{-2} s^{-1}
final irrad. : 5950 uEinstein m^{-2} s^{-1}

flask #	filter	CO (nM)	CO_{avg} (nM)	dCO (nM)	CO_{norm}
initial	---	1.9			
initial	---	1.9	1.9	----	----
initial	---	1.9			
1	n.f.	22.5			
2	n.f.	22.7	22.1	20.2	1.00
3	n.f.	21.0			
4	polycarb.	7.4			
5	polycarb.	6.4	<8.1>	6.2	0.31
6	polycarb.	8.5			
7	y. plex.	4.0			
8	y. plex.	4.2	<4.7>	2.8	0.14
9	y. plex.	4.7			
10	dark	1.8			
11	dark	1.9	1.8	-0.1	----

To augment these results, air equilibrated seawater samples were exposed to a set of more discrete wavebands produced by fluorescent lamps and the same filter materials already described. These samples were poisoned with 140 ppm sodium azide. The spectra from fluorescent "Sunlamps" (FS40), Sunlamps with cellulose acetate and mylar filters, "Black Lamps" (F40BL), and "Cool White" lamps (F40) with polycarbonate and yellow acrylic filters are shown in Figures 15, 16, and 17 respectively. These produce broad wavebands of roughly 275-380 nm, 290-380 nm, 315-380 nm, 295-410 nm, 390-720 nm, and 475-720 nm in addition to the mercury emission peaks at 313 nm, 365 nm, 404 nm, 436 nm, 546 nm, and 578 nm. Longer exposure periods than for the sunlight experiments were needed to produce measurable changes in CO concentrations since the irradiances integrated over the waveband widths ($W\ m^{-2}$) were considerably less, especially in the visible region. Since the spectra were measured at a single point under the fluorescent tubes (see Materials and Methods) they are representative of the spectral distribution experienced by a sample, but not the actual light flux which will be reduced by reflection losses at quartz and filter surfaces, and the rotating position of the flasks. The exposure of each flask was, however, the same.

Two forms of a CO "production efficiency" were defined to help understand the relative effectiveness of the wavebands used. By taking the difference between the light and dark carbon monoxide yields and dividing by the integrated spectral irradiance and duration of exposure (Eq. 6), a carbon monoxide yield relative to the energy of a particular waveband can be calculated. Alternately,

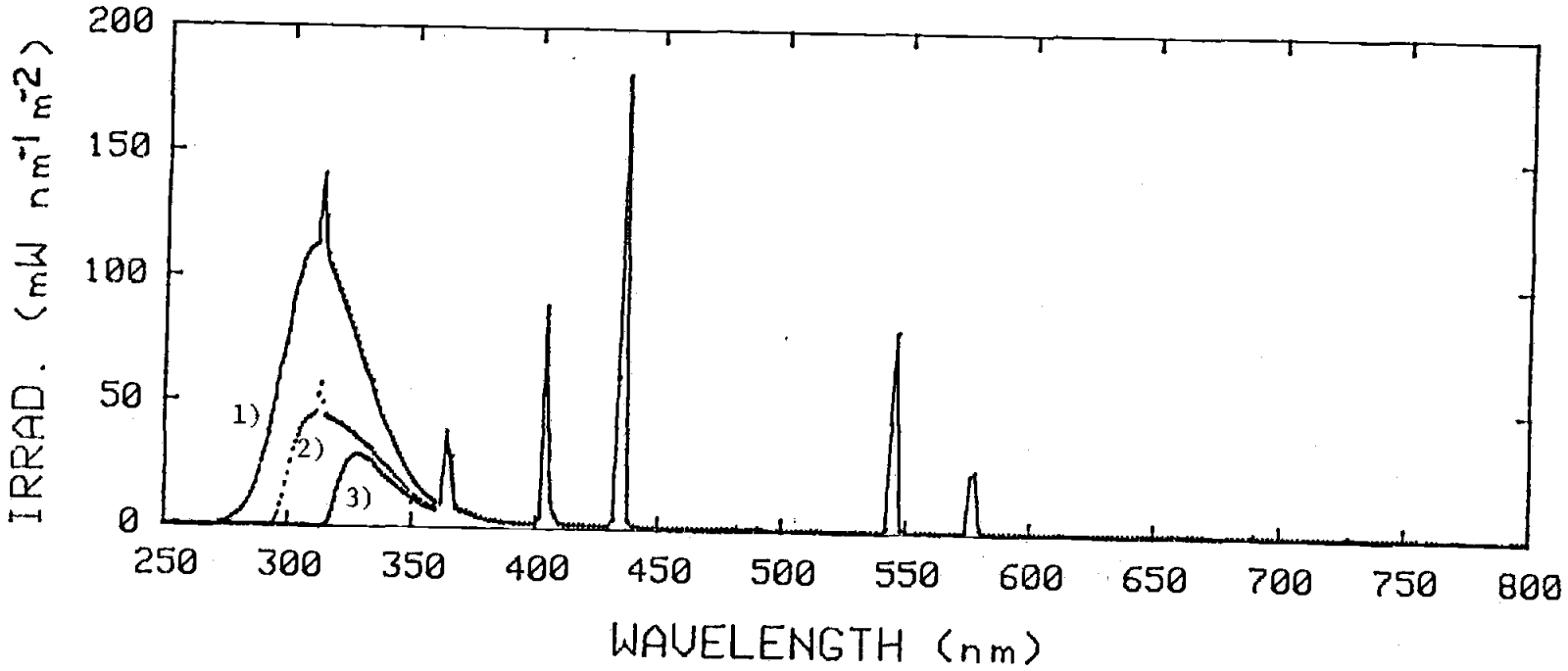

Fig. 15. Spectrum from Westinghouse FS40 fluorescent sunlamps: 1) unfiltered, 2) filtered through cellulose acetate, and 3) filtered through Mylar.

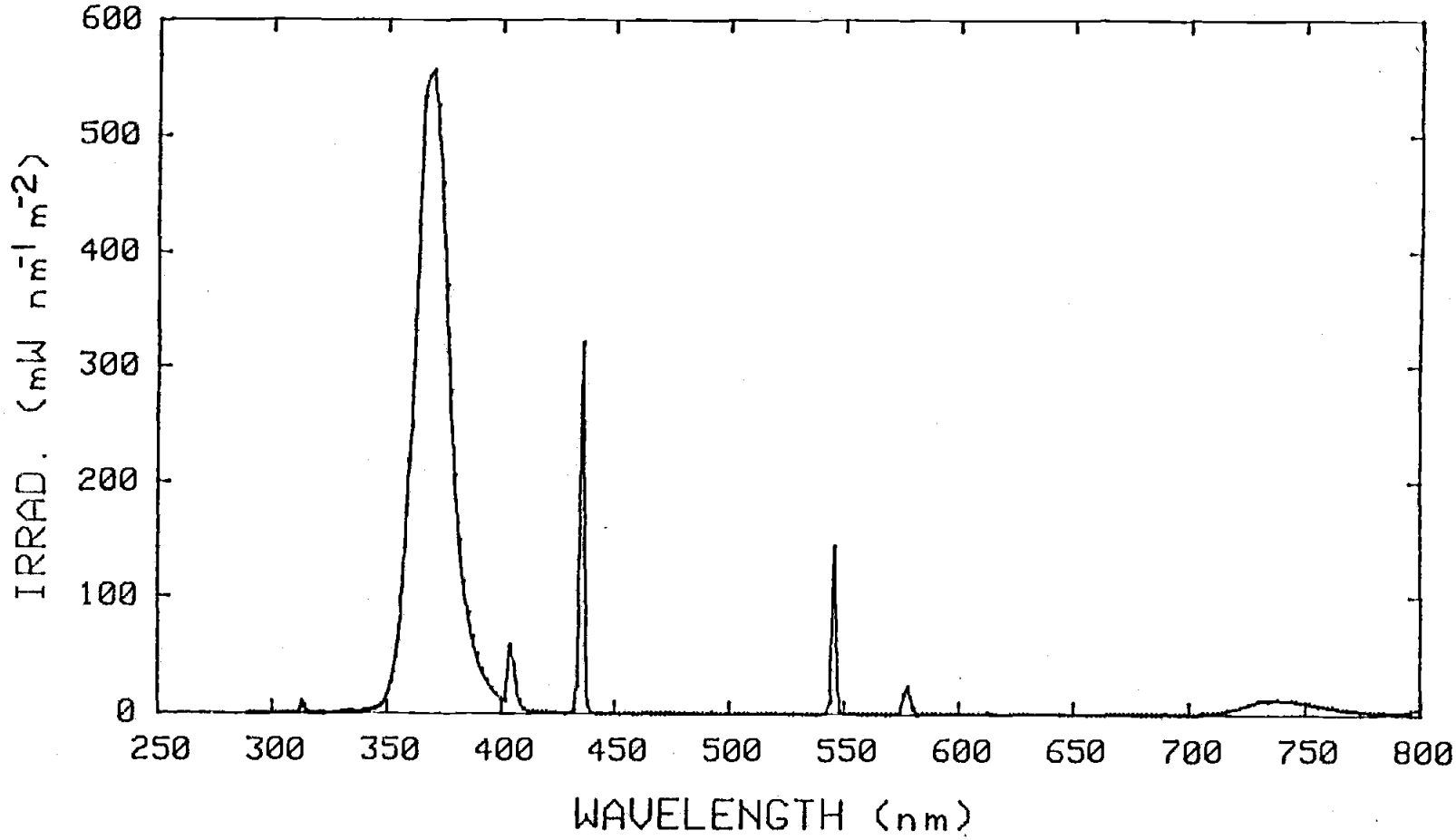

Fig. 16. Spectrum from Westinghouse F40BL fluorescent lamps.

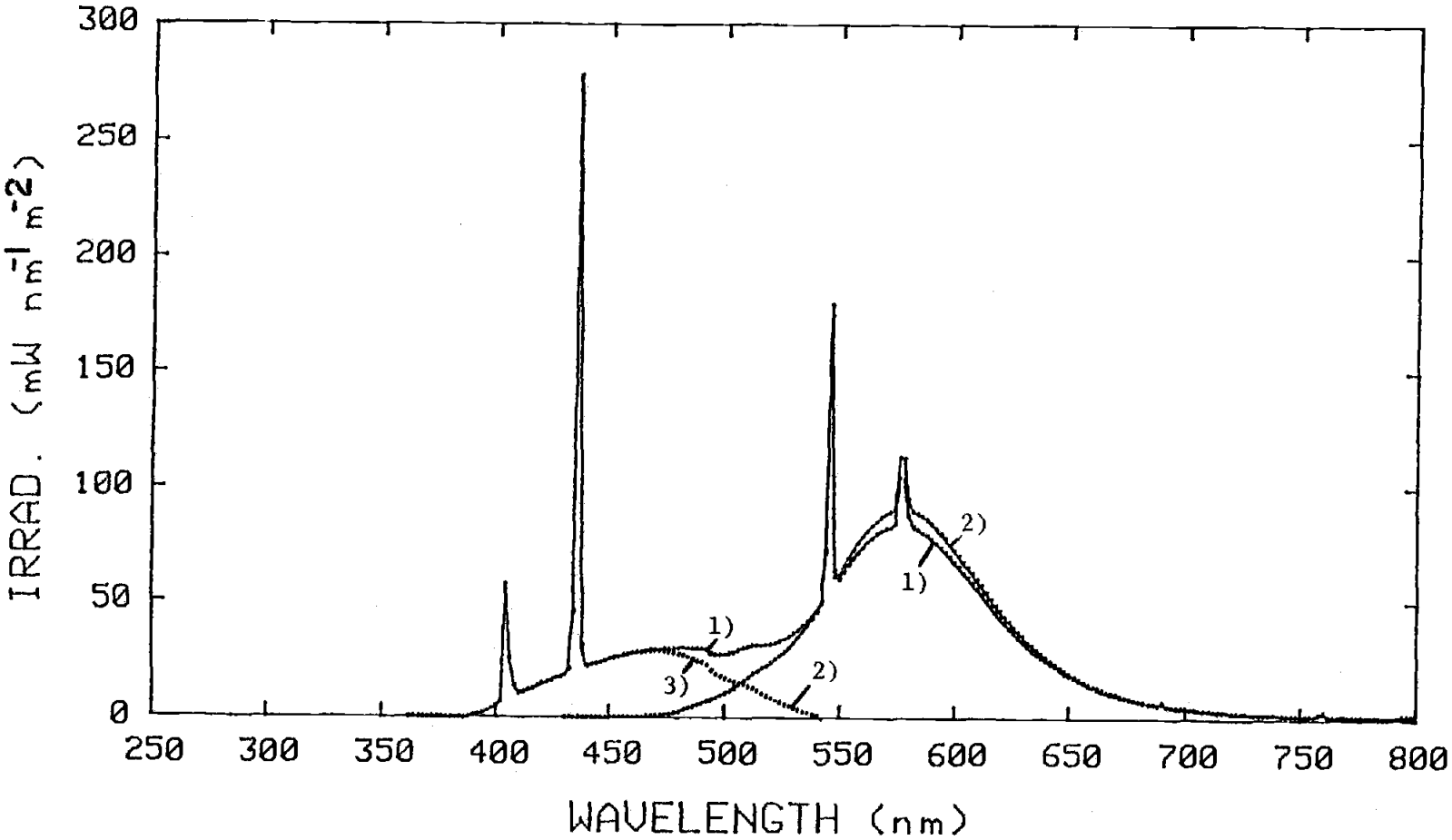

Fig. 17. Spectrum from Westinghouse F40 Cool White lamps: 1) unfiltered, 2) filtered through yellow acrylic plastic, and 3) the difference between 1) and 2).

dividing CO yields by the quantum irradiances and exposure duration (Eq. 7) relates CO production to the photon flux of a particular waveband.

$$\frac{dCO}{I_e \times t} = nM\ CO/(J\ m^{-2}) \qquad (6)$$

$$\frac{dCO}{I_q \times t} = nM\ CO/(uEinsteins\ m^{-2}s^{-1}) \qquad (7)$$

where

$dCO = CO_{exposed} - CO_{dark}$

I_e = integrated irradiance ($W\ m^{-2}$)

I_q = integrated quantum irradiance ($uEinsteins\ m^{-2}s^{-1}$)

t = time (s)

The production efficiency based on photon flux is probably a better description of the relative effectiveness of different wavelengths since most natural photochemical processes are the results of single photon absorption. Both forms, however, are included since most light measurements are reported in terms of energy rather than quanta.

A nominal wavelength of the median energy of each curve was determined. These are listed with the integrated energy of each fluorescent spectrum in Table 5. Results of exposure of seawater to fluorescent lights are listed in Table 6 with the calculated production efficiencies.

The calculated CO production efficiencies were plotted against the nominal wavelengths. This approximates the production of CO per unit energy, or per photon, over the wavelength ranges and is shown in Figure 18. An additional point at 445 nm was determined by

Table 5. Integrated irradiance and nominal wavelength for fluorescent lamp and filter combinations.

LIGHT	FILTER	INTEGRATED IRRADIANCE			
		Watts / m^2	λ,nom. (nm)	ueinsteins / $m^2 s$	λ,nom. (nm)
FS40	n.f.	5.632	320	15.7	323
FS40	cell. acetate	2.786	334	8.22	340
FS40	Mylar	1.719	366	5.42	374
F40BL	n.f.	11.675	370	34.0	370
dF40	*	3.176	452	12.4	456
F40	polycarb.	11.640	560	53.3	568
F40	y. acrylic	8.942	580	43.6	582

*Spectra determined by subtracting F40-y. acrylic, from F40-polycarbonate spectra.

Table 6. CO production in seawater samples exposed to different fluorescent lamp and filter combinations.

FLASK #	LIGHT	FILTER	EXPOSURE TIME (h)	CO (nM)	CO_{avg} (nM)	dCO (nM)	$\frac{dCO}{A^*} \times 10^{+6}$	$\frac{dCO}{B^{**}} \times 10^{+6}$
initial	----	-------	0	0.3				
initial	----	-------	0	0.3				
initial	----	-------	0	0.2	0.3			
initial	----	-------	0	0.3	(0.05)			
initial	----	-------	0	0.3				
1a	FS40	n.f.	6	4.9				
1b	FS40	n.f.	6	4.8	4.8	4.4	36.2	13.0
1c	FS40	n.f.	6	4.7	(0.1)	(0.1)	(0.8)	(0.3)
2a	FS40	acetate	6	2.0				
2b	FS40	acetate	6	2.1				
2c	FS40	acetate	6	2.1	2.1	1.7	28.2	9.6
2d	FS40	acetate	6	2.2	(0.1)	(0.1)	(1.7)	(5.6)
3a	FS40	dark	6	0.4				
3b	FS40	dark	6	0.4				
3c	FS40	dark	6	0.3	0.4	0.1		
3d	FS40	dark	6	0.4	(0.05)	(0.05)		

* $A = (W\ m^{-2}) \times t = J\ m^{-2}$

** $B = (uEinstein/(m2\ s)) \times t = uEinsteins\ m^{-2}$

t = exposure time (s)

() = Standard deviations

Table 6. (cont'd)

FLASK #	LIGHT	FILTER	EXPOSURE TIME (h)	CO (nM)	CO_{avg} (nM)	dCO (nM)	$\frac{dCO}{A^*} \times 10^{+6}$	$\frac{dCO}{B^{**}} \times 10^{+6}$
initial	----	-------	0	0.3				
initial	----	-------	0	0.4	0.3			
initial	----	-------	0	0.3	(0.06)			
4a	FS40	mylar	8	1.3				
4b	FS40	mylar	8	1.4	1.3	1.0	20.2	6.4
4c	FS40	mylar	8	1.3	(0.06)	(0.08)	(1.6)	(0.5)
5a	FS40	dark	8	0.3	0.3	0		
5b	FS40	dark	8	0.3	(0.06)			
initial	----	-------	0	0				
initial	----	-------	0	0				
initial	----	-------	0	0				
6a	F40BL	n.f.	3.5	3.5				
6b	F40BL	n.f.	3.5	3.3				
6c	F40BL	n.f.	3.5	3.3	3.4	2.9	19.7	6.8
6d	F40BL	n.f.	3.5	3.4	(0.1)	(0.1)	(0.7)	(0.2)
7a	F40BL	dark	3.5	0.5	0.5	0.5		
7b	F40BL	dark	3.5	0.4	(0.1)	(0.1)		

Table 6. (cont'd)

FLASK #	LIGHT	FILTER	EXPOSURE TIME (h)	CO (nM)	CO_{avg} (nM)	dCO (nM)	$\frac{dCO}{A^*} \times 10^{+6}$	$\frac{dCO}{B^{**}} \times 10^{+6}$
initial	----	-------	0	0.2				
initial	----	-------	0	0.2	0.2			
initial	----	-------	0	0.2				
8a	F40	polycarb.	17	1.6				
8b	F40	polycarb.	17	1.7				
8c	F40	polycarb.	17	1.6	1.6	1.4	2.0	0.4
8d	F40	polycarb.	17	1.5	(0.1)	(0.1)	(0.3)	(0.03)
9a	F40	dark	17	0.2				
9b	F40	dark	17	0.2	0.2	0		
	dF40		17			1.4	7.2	1.8
initial	----	-------	0	0.1				
initial	----	-------	0	0.1	0.1			
initial	----	-------	0	0.1				
10a	F40	y.plex.	17	0.2				
10b	F40	y.plex.	17	0.2				
10c	F40	y.plex.	17	0.1	0.2	0	0	0
10d	F40	y.plex.	17	0.1	(0.1)			
11a	F40	dark	17	0.2				
11b	F40	dark	17	0.1	0.2	0.1		

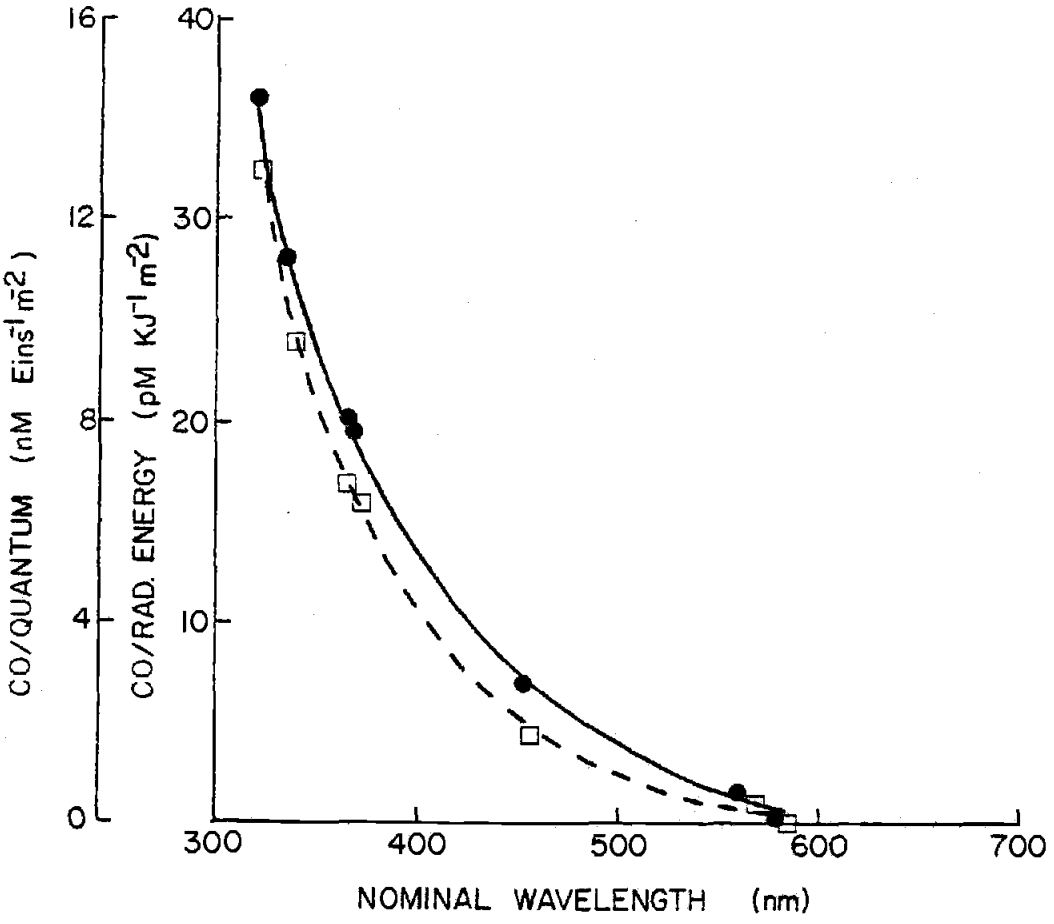

Fig. 18. CO production efficiencies vs nominal wavelength for spectra. Circles are CO (rad. energy)$^{-1}$, and squares are CO (quantum irrad.)$^{-1}$.

subtracting the spectra of F40 lamps with yellow acrylic from that of F40 lamps without filters, determining the nominal wavelength of the resulting spectral curve, and assuming that all CO production occured within this waveband. This was considered valid since production of CO was not observed when using light from F40 lamps that was filtered through yellow acrylic. Therefore light between 400 and 500 nm (the difference between the spectra) was probably responsible. These calculations do not determine true quantum yields in a photochemical sense, but do demonstrate differences between long and short wavelength radiation on CO production.

C. Photoproduction of CO In Poisoned, Autoclaved, and Filtered Seawater Samples

In previous experiments, the intensity of sunlight and presence of relatively high fluxes of ultraviolet radiation may have been sufficient to inhibit microbial activity that would otherwise affect the concentration of CO (Smith et al., 1980; Lorenzen, 1979; Worrest et al., 1978; Baker et al., 1980). This is supported by the stability of CO concentrations following exposure in this work. This also contrasts with experiments by Conrad and Seiler (1980a) where CO consumption was observed in seawater (in glass bottles) incubated both under sunlight and in the dark. Since direct methods to verify sterility of the samples were not used, additional experiments were done with the initial purpose of testing abiotic production or consumption of CO.

Sodium azide and mercuric chloride were considered for poisoning

experiments since they were not organic or volatile (volatile organic compounds were found to be incompatible with the gas chromatographic system). Both of these compounds are widely used to inhibit microbial activity in natural samples (Bullister et al., 1981; Conrad and Seiler, 1980a).

Sodium azide was added to five flasks with seawater resulting in an azide concentration of approximately 140 ppm. Three of these were exposed to sunlight for 1 h along with three flasks that were not poisoned. Two poisoned samples, and two untreated samples were kept covered to check for dark changes in the CO concentration. As shown in Table 7, there was little difference in CO production between untreated and poisoned seawater samples.

A second set of samples was prepared in a similar manner using mercuric chloride at a concentration of 100 ppm as a poison. The results are also listed in Table 7. Samples treated with mercury yielded significantly higher amounts of CO relative to untreated water. This same effect had been observed in other experiments not included here and it is possible that mercury was acting to sensitize the photo-production of CO. There are several examples of mercury sensitization of photochemical reactions in the literature that support this explanation (Coxon and Halton, 1974). An alternate explanation would be reduction of microbial uptake of CO, but this is not likely since initial experiments demonstrated that CO concentrations remained constant when samples were removed from the light. The results of adding mercuric chloride is an interesting example of a possible matrix effect on a photochemical process.

Seawater samples were autoclaved as an additional check of

Table 7. CO production in seawater samples poisoned with sodium azide or mercuric chloride.

Initial irrad.: 4400 uEinstein m^{-2} s^{-1}
Final irrad. : 5400 uEinstein m^{-2} s^{-1}

Flask #	Treatment	Exposure (hr)	CO (nM)	CO_{avg} (nM)	dCO (nM)
init.	none	0	0.6		
init.	none	0	0.5	0.6	---
init.	none	0	0.6	(0.06)	
1	none	2	18.8		
2	none	2	21.2	20.5	19.9
3	none	2	21.6	(1.5)	(1.5)
4	azide*	2	20.6		
5	azide	2	22.6	21.5	20.9
6	azide	2	21.2	(1.0)	(1.0)
7	azide	dark	0.6		
8	azide	dark	0.5	0.5	-0.1
9	none	dark	0.6		
10	none	dark	0.4	0.5	-0.1
init.	none	0	0.6		
init.	none	0	0.5	0.5	---
				(0.07)	
1	none	2	29.4		
2	none	2	30.0	29.0	28.5
3	none	2	27.7	(1.2)	(1.2)
4	$HgCl_2$**	2	46.2		
5	$HgCl_2$	2	46.9	46.1	45.6
6	$HgCl_2$	2	45.2	(0.9)	(0.9)
7	$HgCl_2$	dark	0.9	0.8	0.3
8	$HgCl_2$	dark	0.6	(0.2)	(0.2)
9	none	dark	0.7	0.6	0.1
10	none	dark	0.4	(0.2)	(0.2)

* Sodium azide concentration = 140 ppm
** Mercuric chloride concentration = 100 ppm
() indicates standard deviations

sterility. Four flasks were filled with water samples that were stripped with nitrogen prior to autoclaving to lower the oxygen concentrations. Four flasks were filled with seawater that had been air equilibrated and autoclaved, and three flasks were filled with untreated seawater. These flasks were then exposed to sunlight for 2 h.

Production of carbon monoxide in these samples is listed in Table 8. The nitrogen stripped/autoclaved samples, and the untreated samples yielded less CO than samples that had not been stripped prior to autoclaving, although CO production was still greater than untreated samples. It appears that CO producing substrates are created during autoclaving and that oxygen is a reactant. (Note that the oxygen concentrations are low, but not zero at the time of analysis.) Carbon monoxide was also generated during autoclaving, possibly by the thermal oxidation of organic species.

D. Influence of Dissolved Oxygen on Photochemical Production of Carbon Monoxide

To test the influence of oxygen on production of CO, seawater samples were prepared with varying concentrations of O_2. This was done using the apparatus shown in Figure 7. In the first experiment, water samples were either: 1) purged of oxygen by bubbling dispersed nitrogen through the sample, 2) enriched in oxygen by bubbling O_2 through the sample, or 3) air equilibrated. Three sets of flasks were filled with each of these sample types, exposed to sunlight, and analysed for CO and O_2.

In a second experiment, which was repeated, seawater was

Table 8. CO production in autoclaved, stripped/ autoclaved, and untreated seawater.

Initial irrad: 5500 uEinstein m^{-2} s^{-1}
Final irrad: 4680 uEinstein m^{-2} s^{-1}

Flask #	Treatment*	Exposure (h)	CO (nM)	CO_{avg} (nM)	dCO (nM)	O2 (uM)
init.	none	0	3.8			256
init.	none	0	3.8	3.8	---	262
init.	N_2	0	0			3
init.	N_2	0	0	0		3
1	none	2	32.3			
2	none	2	31.8	31.9	28.1	242
3	none	2	31.7	(0.3)	(0.3)	247
4	Auto	0	7.4	7.4		154
5	Auto	2	54.2			151
6	Auto	2	54.9	53.5	46.1	136
7	Auto	2	51.3	(1.9)	(1.9)	136
8	N_2,Auto	0	1.5	1.5		72
9	N_2,Auto	2	35.6			129
10	N_2,Auto	2	34.5	35.7	34.2	116
11	N_2,Auto	2	37.1	(1.3)	(1.3)	118

*N_2: Nitrogen stripped
Auto: Autoclaved
(): standard deviations

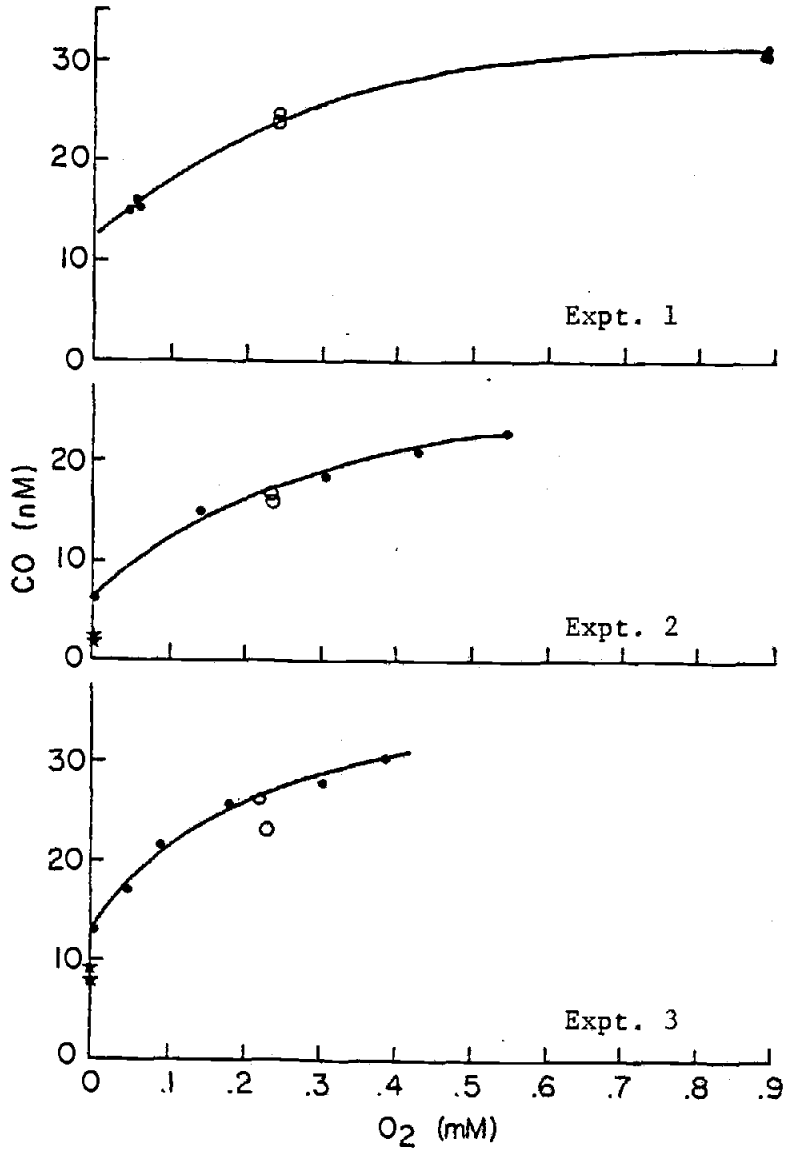

Fig. 19. CO production in seawater samples exposed to sunlight, with varying O_2 concentrations. Closed circles: O_2 conc. adjusted by purging. Open circles: Air-equilibrated. Stars: Sodium sulfite added.

consistent with that of the other samples (with a single exception). Also, CO is still produced in the apparent absence of oxygen. Where sodium sulfite was added to remove oxygen, CO production still occurred, but was lower than that of water samples that were stripped of oxygen using nitrogen. Production was also lower than predicted by extrapolating the curves to zero O_2.

E. CO Production From Added Substrates

A suite of compounds was chosen to test potential substrate materials and mechanisms for carbon monoxide production in seawater. These were: Acetone, acetaldehyde, acetic acid, methanol, urea, dextrose, and humic acid. Although clearly not an exhaustive list, these were chosen for a number of reasons. The primary criterion was that each could be considered representative of organic functional groups that are common in marine dissolved organic matter, and are potential sources for carbon monoxide. Also, each compound is a known component of seawater (Duursma, 1965; Corwin, 1970; McCarthy, 1970) especially humic acid which probably is most representative of the bulk of dissolved organic matter. Finally, by using some soluble low molecular weight compounds, (acetone, acetaldehyde, etc.) it was possible that methane, as a possible photochemical product could be detected, which would indicate a possible CO source mechanism.

Each of the test compounds were added directly to quartz flasks along with air equilibrated seawater. The flasks were then exposed in the usual manner, and the results are listed in Tables 9, 10, and

11. Lower concentrations of each compound were also tested, but only those concentrations which provided easily recognizable results against the background of CO produced by seawater are listed.

Acetone, acetaldehyde, and humic acid all clearly yielded carbon monoxide. Urea, methanol, acetic acid, and dextrose did not produce measurable amounts of CO at the concentrations used. Acetaldehyde yielded 3 to 4 times more CO per mole than did acetone. Humic acid produced roughly 1100 times more CO per mg than acetone.

In addition to CO, acetone, and acetaldehyde also yielded measurable amounts of methane; however, the methane produced was only a small fraction (5 and 6% respectively) of the CO produced in each case. Acetaldehyde yielded approximately four times as much methane per mole as did acetone. Methane production in seawater with added humic acid was not observed.

Table 9. CO production from acetone, acetaldehyde, and acetate added to seawater.

Exposure period: 1.5 hr
Initial irrad.: 4510 uEinstein m^{-2} s^{-1}
Final irrad.: 5620 uEinstein m^{-2} s^{-1}

NO.	SAMPLE	CONC. (mM)	CO (nM)	CO_{avg} (nM)	dCO (nM)	$\frac{dCO}{CONC}$ $x10^{+3}$	CH_4 (nM)	CH_4 (nM)	dCH_4 (nM)	$\frac{dCH_4}{CONC}$ $x10^{+3}$
init.	SW		0.8				3.4			
1	SW		37.0				3.0			
2	SW		34.2	35.6			3.3	3.2		
				(2.0)				(0.2)		
init.	SW+acetone	4.4	0.9				3.4			
3	SW+acetone	4.4	52.0				3.7			
4	SW+acetone	4.4	46.4	48.6	13.0	3.0	4.0	3.9	0.7	0.16
5	SW+acetone	4.4	47.4	(3.0)	(3.6)		4.1	(0.2)	(0.3)	
init.	SW+acetaldehyde	5.7	0.9				3.4			
6	SW+acetaldehyde	5.7	102				6.5			
7	SW+acetaldehyde	5.7	99.3	98.5	62.9	11.0	7.0	6.9	3.7	0.65
8	SW+acetaldehyde	5.7	94.2	(4.0)	(4.2)		7.3	(0.4)	(0.5)	
init	SW+acetate	10.5	0.8				3.3			
9	SW+acetate	10.5	38.4				3.3			
10	SW+acetate	10.5	33.9	35.4	-0.2	---	3.2	3.3	0.1	0.01
11	SW+acetate	10.5	33.8	(2.6)	(3.3)		3.3	(0.1)	(0.2)	

Table 10. CO production from urea and dextrose added to seawater.

Exposure period: 1.5 h
Initial irrad.: 5450 uEinstein m^{-2} s^{-1}
Final irrad.: 4450 uEinstein m^{-2} s^{-1}

NO.	SAMPLE	CONC. (mM)	CO (nM)	CO (nM)	dCO (nM)	$\frac{dCO}{CONC}$ $x10^{+3}$	CH_4 (nM)	CH_4 (nM)	dCH_4 (nM)	$\frac{dCH_4}{CONC}$ $x10^{+3}$
init.	SW		0.9				3.6			
1	SW		19.6				3.5			
2	SW		19.5	19.9			3.7	3.6		
3	SW		20.7	(0.7)			3.6	(0.1)		
init.	SW+urea	16.7	1.0				3.6			
4	SW+urea	16.7	19.5				3.6			
5	SW+urea	16.7	19.9	19.7	-0.2	---	3.6	3.6	0	0
6	SW+urea	16.7	19.7	(0.1)	(0.7)		3.5	(0.1)	(0.1)	
init.	SW+dextrose	5.4	1.0				3.6			
7	SW+dextrose	5.4	19.2				3.6			
8	SW+dextrose	5.4	22.6	20.8	0.9	0.2	3.6	3.6	0	0
9	SW+dextrose	5.4	20.7	(1.7)	(1.8)		3.6			

Table 11. CO Production from humic acid and acetone added to seawater.

Exposure period: 1.6 h
Initial irrad.: 4620 uEinstein m^{-2} s^{-1}
Final irrad.: 5820 uEinstein m^{-2} s^{-1}

NO.	SAMPLE	CONC. (mg l^{-1})	CO (nM)	CO (nM)	dCO (nM)	dCO CONC (nmol mg^{-1})	CH_4 (nM)	CH_4 (nM)	dCH_4 (nM)	dCH_4 CONC (nmol mg^{-1})
init.	SW		1.9				3.1			
1	SW		52.1				3.3			
2	SW		52.8	52.5			3.2	3.2		
3	SW		52.6	(0.4)			3.2	(0.1)		
init.	SW+humic acid	1.14	1.9				3.1			
4	SW+humic acid	1.14	165				3.3			
5	SW+humic acid	1.14	170	168	115	101	3.2	3.2	0	0
6	SW+humic acid	1.14	168	(2.5)	(2.5)		3.1	(0.1)	(0.1)	(0.1)
init.	SW+acetone	255	1.9				3.1			
7	SW+acetone	255	74.2				3.5			
8	SW+acetone	255	75.0	74.6	22.1	0.09	3.6	3.5	0.3	1.2×10^{-3}
9	SW+acetone	255	74.7	(0.4)	(0.6)		3.4	(0.1)	(0.1)	

VI. DISCUSSION

The first experiment demonstrated that photo-production of carbon monoxide was directly related to the flux of sunlight to which the samples were exposed. It was also found that when exposed samples were removed from sunlight, CO concentrations remained constant for a period of at least six hours.

These results have several implications. For subsequent experiments, it was assumed that CO concentrations in the flasks remained constant after a period of exposure before analysis of the dissolved gases was done. This is especially important since, as was pointed out, the final CO concentrations were usually highly supersaturated relative to atmospheric concentrations. It appears that the concentration of the precursor for CO production is not reduced to an extent great enough to curtail linear production during the five hour period.

The finding that CO levels remain constant after light is removed contrasts with experiments performed by Conrad and Seiler (1980a). In their report, CO concentrations were monitored in seawater samples that were collected in glass containers and incubated under natural illumination. The concentration of CO was found to decrease with decreasing light intensity, and the change in concentration seemed to lag behind the change in light intensity. However, samples that were poisoned with sodium azide (at a concentration of 200 ppm) were said to show linear production of CO over a period of 16 h (morning to evening) even though the natural light intensity was following a normal daily cycle. In fact, CO

production continued after the light had disappeared. Based on these results, it was proposed that CO was produced photochemically by a "delayed reaction" and that CO was consumed microbially.

Microbial consumption of CO concentrations in surface waters (with time and depth) following peak light levels, is consistent with studies that have demonstrated several biologic mechanisms by which CO could be metabolized. However, results of the first experiment presented here seem to indicate that a consumptive process during this study was not active since loss of CO after exposure was not observed.

Using small diameter quartz flasks may have resulted in exposure of the water samples to visible and UV light fluxes much greater than would be expected for water in a mixed system, or at greater depth in a water column. This is especially true of ultraviolet light which would normally be attenuated by chlorophyll and dissolved organic matter (Smith and Baker, 1979). Several studies have demonstrated the adverse affects of high intensity visible and ultraviolet light on marine organisms (Lorenzen, 1979; Calkins and Thordardottir, 1980; Worrest et al., 1978; Steemann Nielsen, 1974). These suggest that microbial activity, if initially present, could have been inactivated or suppressed. If photoinhibition did occur, however, it would not be entirely due to ultraviolet light since samples that were exposed to light filtered through a polycarbonate filter also showed constant CO concentrations after exposure. Polycarbonate absorbs most ultraviolet light, and all UV-B (see Figure 14). It should be pointed out that in Conrad's experiments, glass containers were used, and these were immersed (it is assumed) in a seawater bath for

temperature control. Both glass and seawater could somewhat attenuate the ambient ultraviolet light that reached the samples.

By using a water bath, Conrad and Seiler's samples were kept at roughly the same temperature (28 C) as the sample location. This should improve chances that the microbial communities in the sample would remain viable. In the experiments presented in this study, the temperature was not controlled. Seawater samples were approximately 9 C when collected and attained temperatures between 25 C and 32 C during exposure to sunlight. This was not considered a problem for the type of general photochemical information that was being sought, although it may have affected (fortuitously) the microbial activity of the samples. Alternate explanations are: 1) Low initial populations of CO consuming organisms, 2) slow adaptation to higher CO levels, or 3) inhibition by the toxic effects of high levels of CO.

As noted, Conrad and Seiler concluded that since peak concentrations of CO measured in surface waters occur after peak light intensities, then CO must be produced by a delayed reaction mechanism. This was also inferred from results of their incubation experiments where linear CO production continued in low (or no) light. The implication is that light absorption photochemically produces unstable intermediate products which subsequently undergo light independent reactions that are slow, diffusion controlled processes. The results of the exposure experiment here, however, suggest that the photochemical production of CO in these samples was a relatively fast reaction since CO does not continue to increase after removing the samples from sunlight.

This does not exclude the possibility that CO may be produced by secondary rather than primary processes. But these processes, if diffusion controlled, would be much quicker than Conrad and Seiler's results suggest. If secondary reactions were producing CO, the reactions were essentially complete in less than 10 minutes while the data from Conrad and Seiler's experiments showed continuing production for several hours after the light had disappeared. An explanation for this difference is not known, unless much longer exposure times, or exposure to different light spectra, are required to produce a significant concentration of reactive intermediates. Diffusion in the dissolved or particulate content of the samples could also be a factor.

Nevertheless the time delay of CO production behind light intensity does not necessarily indicate a delayed reaction is taking place. This can be demonstrated with a simple model. As a first approximation, it is assumed that CO is produced only by a photochemical process, and a consumption process exists which may or may not be dependent on the concentration of CO. For this model, it is assumed that CO production is instantaneous and dependent directly on light intensity. For simplicity, diffusion, advection, and wavelength contributions are not included.

Three possible modes of CO consumption are considered. The first assumes that consumption simply occurs at a constant rate and is independent of the concentration of CO (a zero order reaction). The second assumes a first order consumption process that is directly proportional to the CO concentration. The third assumes a second order process where consumption is proportional to the square of the

CO concentration. The three cases are given by the following equations:

$$d(CO)/dt = K_1(I) - K_2 \quad (8)$$

$$d(CO)/dt = K_1(I) - K_3(CO) \quad (9)$$

$$d(CO)/dt = K_1(I) - K_4(CO)^2 \quad (10)$$

where I is the light intensity and K_1 is a production rate constant. Consumption rate constants are K_2, K_3, K_4 for each of the respective cases.

The light intensity, I, can be approximated by a simple sine function, $I_o \sin(ct)$, to describe the changing light intensity during a day. I_o is the maximum light intensity at solar "noon", and c is a constant to convert time (t) to units of degrees (or radians). Solar noon would occur at 90 degrees, and sunrise and sunset would occur approximately at 0 and 180 degrees respectively. A sine function approximation of the light intensity is reasonable when compared to the calculated subsurface UV-B dose rates reported by Smith and Baker (1979).

The equations become:

$$d(CO)/dt = K_1(I_o \sin(ct)) - K_2 \quad (11)$$

$$= K_1(I_o \sin(ct)) - K_3(CO) \quad (12)$$

$$= K_1(I_o \sin(ct)) - K_4(CO)^2 \quad (13)$$

A final variation of this model is to induce a delay in the consumption rate expression of equation (13) by modifying

$K_4(CO)^2$ to $K_4(CO_{t-x})(CO)$. This can be interpreted as an approximation of an "adaptive" process whereby the capacity of the consumption process (e.g. an organism) to consume CO, $K_4(CO_{t-x})$, requires x amount of time to adapt to the concentration it experiences at time t-x.

Carbon monoxide production curves were computed by finite-difference using 0.1 deg increments, and;

$$CO = 0.1\left(\sum_{0}^{i} \frac{dCO}{d(ct)}\right)_i \qquad (14)$$

where $i = (ct)/0.1$. K_1 through K_4 were assigned arbitrary values to generate families of curves within the same scale as light intensity. For simplicity, $I_o = 1$ and $0 < (ct) < 180$ degrees. The results are shown in Figures 20-23.

Note that maximum CO concentrations using equations (11) and (12) always occur after peak light intensity even though CO production was instantaneous. In the third case (Eq. 13), the maximum concentrations of CO may occur prior to or following peak light intensity depending on the relative magnitude of the rate constants, K_1 and K_4, and the length of adaptive time delay (x).

A delayed reaction, therefore, is not required, to explain the apparent lag of CO production. A slow reaction, on the other hand, could accentuate the difference between the CO and light intensity curves. Examples of diuranl changes in CO concentrations measured at two locations (Seiler and Schmidt, 1974; Linnenbom, et.al., 1973) are shown in Figures 23 and 24 for comparison.

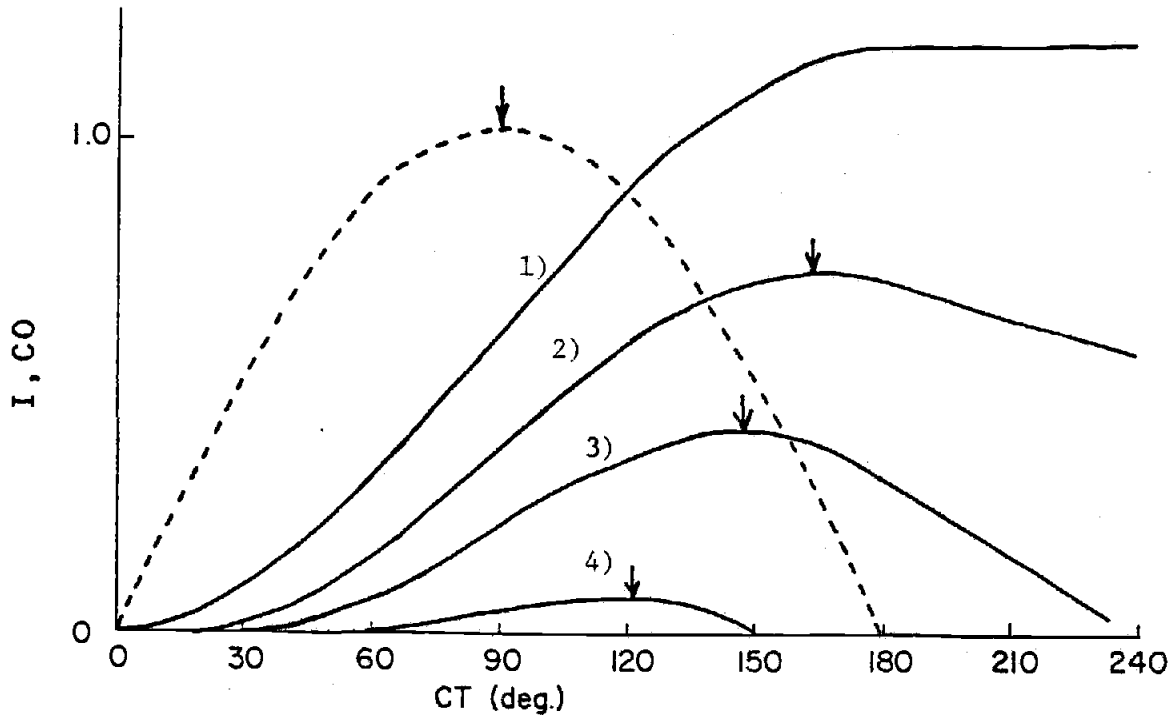

Fig. 20. Model of CO production relative to light intensity (dashed line) based on Eq. 11 .

1) $K_1 = 0.01$, $K_2 = 0$

2) $K_1 = 0.01$, $K_2 = 0.0025$

3) $K_1 = 0.01$, $K_2 = 0.005$

4) $K_1 = 0.01$, $K_2 = 0.0087$

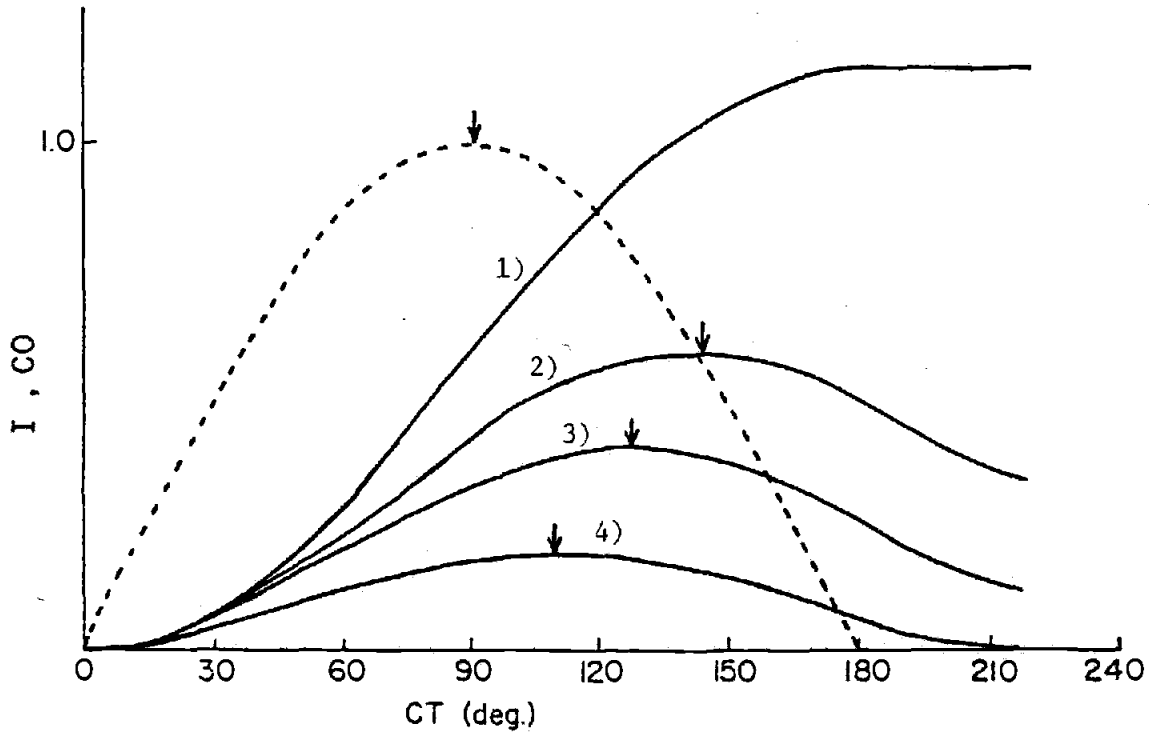

Fig. 21. Model of CO production relative to light intensity (dashed line) based on Eq. 12.

1) $K_1 = 0.01$, $K_2 = 0$

2) $K_1 = 0.01$, $K_2 = 0.01$

3) $K_1 = 0.01$, $K_2 = 0.02$

4) $K_1 = 0.01$, $K_2 = 0.05$

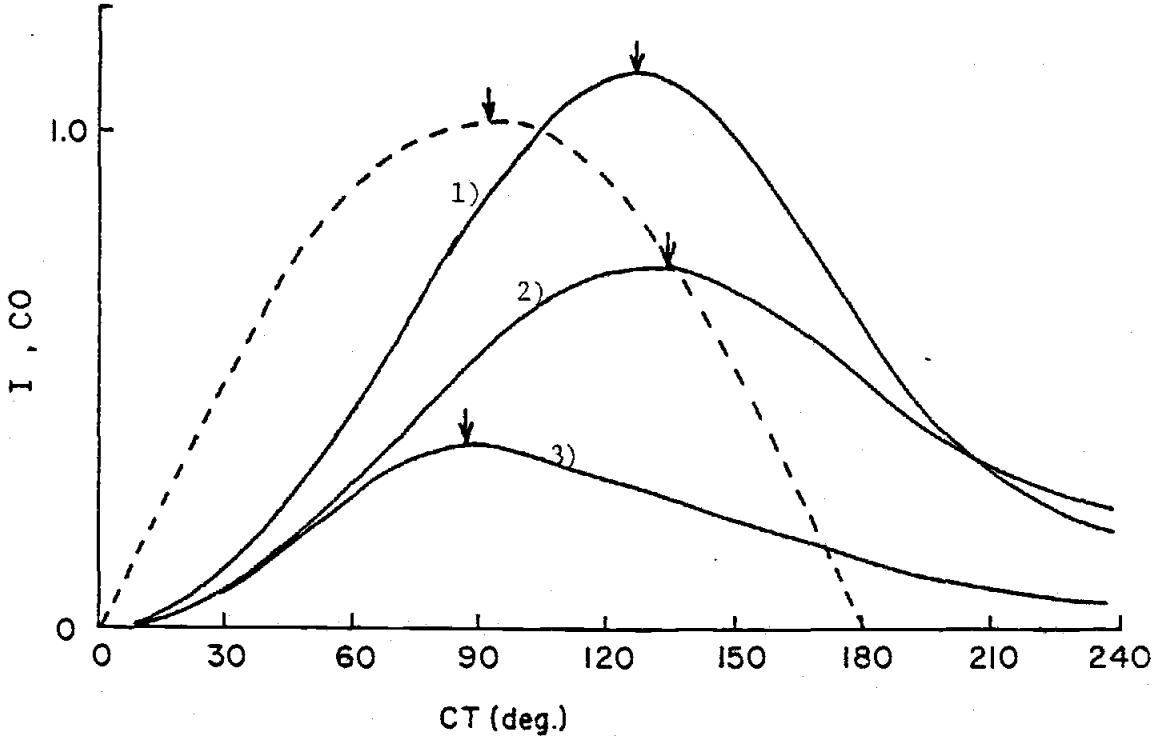

Fig. 22. Model of CO production relative to light intensity (dashed line) based on Eq. 13 modified for delayed consumption.

1) K_1= 0.02, K_2= 0.02, delay(x)= 45 deg

2) K_1= 0.01, K_2= 0.02, delay= 45 deg

3) K_1= 0.01, K_2= 0.10, delay= 30 deg

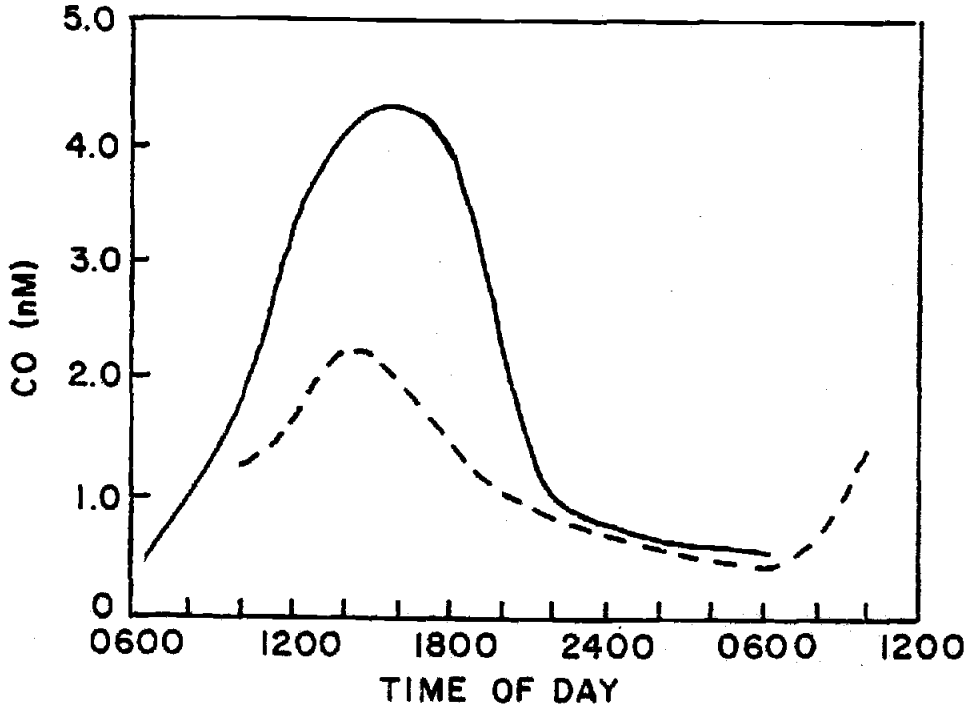

Fig. 23. Carbon monoxide concentrations in surface water at two locations of the North Atlantic vs time of day (adapted from Linnenbom et al. 1973).

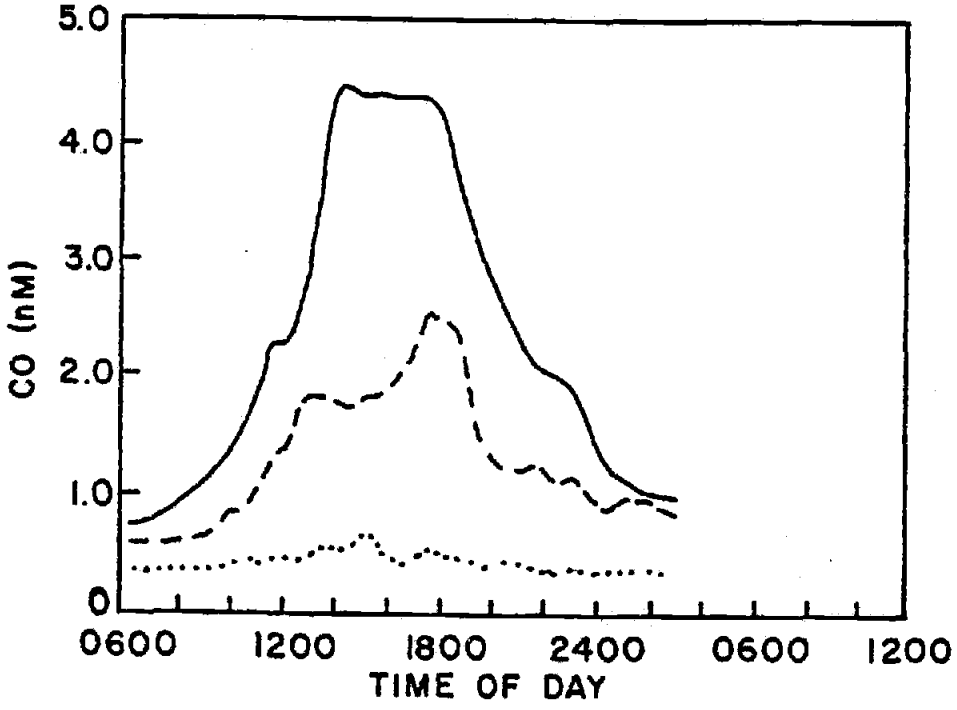

Fig. 24. Carbon monoxide concentrations in surface water of the Gulf of Cadiz vs time of day: 1) clear sky, 2) broken clouds, and 3) overcast. (adapted from Seiler and Schmidt, 1974).

Ultraviolet radiation was found to be most effective per unit energy, or per photon, for producing CO in seawater. It appears, however, that CO production is not dependent on discrete wavelengths, and visible light can result in CO production, although with lower efficiency.

In Figure 25, CO production efficiencies based on relative quantum flux are plotted on a log scale against wavelength, and the result is a linear relationship. It is interesting to compare this with the absorbance for marine "Gelbstoff" (yellow substance) in Figure 5. The relation between absorbance and wavelength is of the form $\log a(\lambda) = C + K(\lambda)$ where $a(\lambda)$ is the absorbance at the wavelength λ, C is a constant related to the concentration of dissolved organic matter, and K is the slope of the line which is dependent on the nature of material. In a recent study by Bricaud et al. (1981), spectral absorbances were determined for a variety of water samples with a wide range of dissolved organic matter concentrations. In the 290-600 nm range, the linear relation was confirmed, and the slope was found to be approximately constant ($K = -0.015$). Note that CO production and "Gelbstoff" absorbance are both linear and span roughly two orders of magnitude between 290-600 nm. This suggests that CO production is directly related to absorption of light by the largely undefined Gelbstoff fraction of dissolved organic matter. "Gelbstoff" may therefore be a primary source of CO as opposed to specific dissolved compounds.

It appears that wavelengths greater than 400 nm (visible light) are active in CO production. This is supported by the observation from the solar spectrum experiments that sunlight filtered through

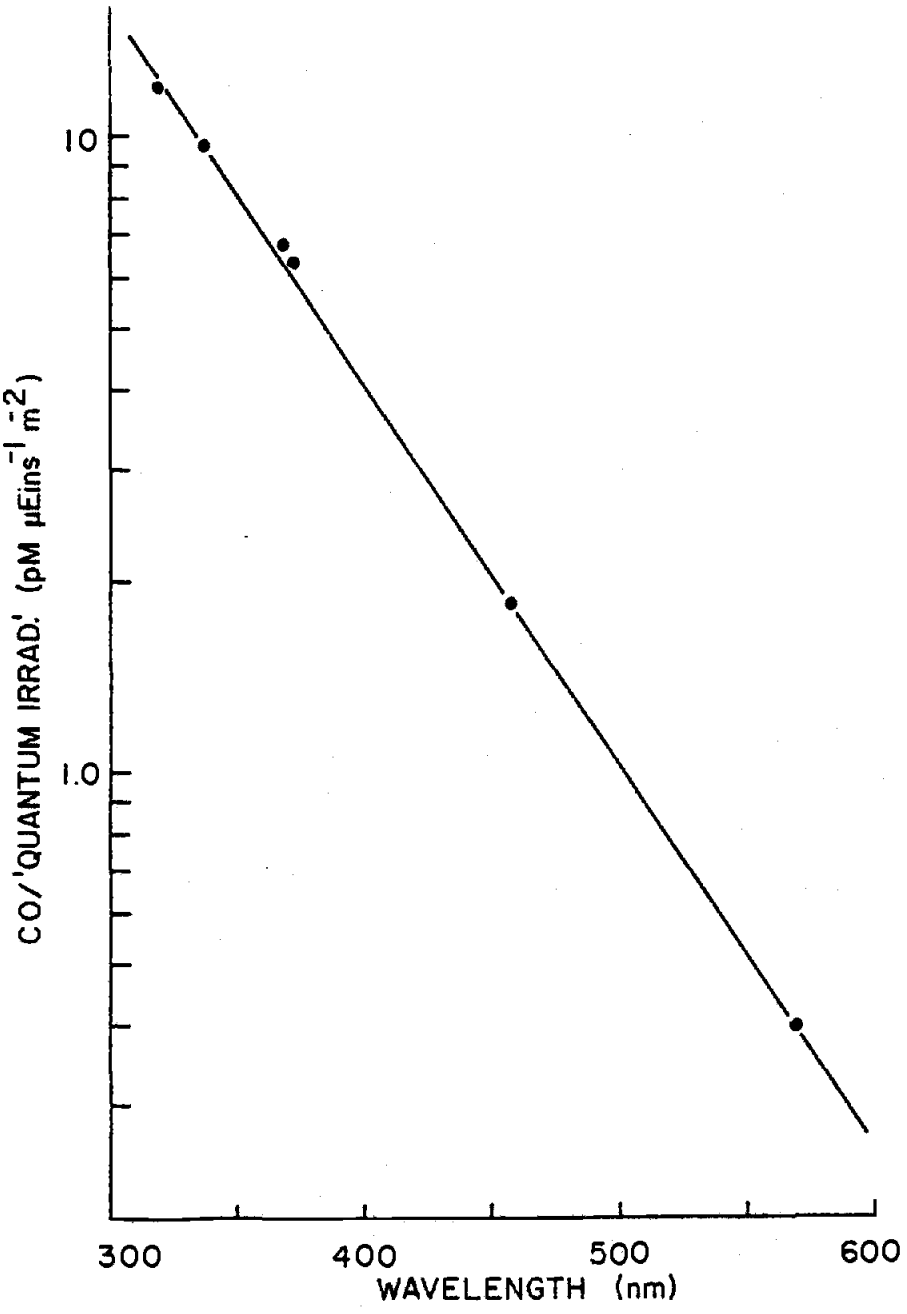

Fig. 25. Carbon monoxide production efficiencies plotted on a logarithmic scale vs wavelength.

yellow plexiglass (no significant light below 465 nm) also produced CO. The reason that the fluorescent spectrum of F40 lamps combined with yellow acrylic filter did not produce measurable CO could be a result of the much lower intensity light, or light in the region of 470 nm which was present in the solar spectrum but not in the fluorescent spectrum.

The concentration of carbon monoxide has been observed to follow a diurnal cycle throughout the euphotic zone (Seiler and Schmidt, 1974). The largest variations occur near the surface and decrease to an apparently constant level below the euphotic zone. Since ultraviolet radiation is attenuated to approximately 1% within the upper 10% of the euphotic zone, it is logical that maximum production would occur at the surface. In addition it was pointed out earlier that clear seawater acts as a crude monochromator transmitting predominantly blue and near ultraviolet light. Therefore, it is possible for CO to be photochemically produced to the extent of light penetration depending on the presence of substrate material and absorbing species. The photochemical process would be superimposed on other factors such as diffusion, advective mixing, and non-photochemical or biological processes.

To summarize the findings:

1) Photochemical yield of CO increases with increasing concentrations of dissolved oxygen. The relationship, however, is not linear. Carbon monoxide production becomes less dependent on oxygen at higher oxygen concentrations.
2) Carbon monoxide can be produced in the apparent absence of

oxygen.

3) When oxygen was removed chemically using sodium sulfite, the production of CO was less than in samples that were stripped of oxygen using nitrogen. Production was also less than would be predicted by extrapolating the CO vs. oxygen curves to zero oxygen.

4) Seawater that had been stripped with nitrogen and autoclaved yielded CO at a rate lower than that of air-equilibrated seawater that had been autoclaved.

5) Carbon monoxide production in seawater increased when mercuric chloride was added.

6) Carbon monoxide production increased in seawater when acetone, acetaldehyde, or humic acid were added. Carbonyl functional groups are present in each of these substrates. Other substrates tested did not have these groups, and did not affect CO production.

7) In addition to CO, methane was produced in seawater when acetone or acetaldehyde were added. These were the only cases among all the experiments where methane was found to change significantly after exposure to light.

8) Dissolved humic acid was capable of producing CO at approximately 1100 times the rate for acetone on a weight-concentration basis.

Using the relationships observed in this study between CO production, dissolved oxygen concentration, and representative substrate compounds, it is possible to propose a mechanism for

photochemical production of CO in seawater.

One mechanism that is consistent with these observations is photoelimination of carbonyl functional groups from relatively complex organic matter. Oxygen may react photochemically to oxidize organic matter and thereby increase the concentration of carbonyl groups.

Formation of methane in samples with acetone, CH_3-CO-CH_3, or acetaldehyde, CH_3-CHO, is probably the result of reactions that follow carbon-carbonyl bond cleavage (Norrish Type I fragmentation; Hoorspool, 1976). A methyl radical is formed initially which can abstract hydrogen from a number of sources to form methane:

$$(CH_3,H)-\overset{O}{\overset{\|}{C}}-CH_3 \xrightarrow{h\nu} (CH_3,H)-\overset{O}{\overset{\|}{C}}\bullet + \bullet CH_3 \qquad (15)$$

$$\bullet CH_3 + HR \longrightarrow CH_4 + \bullet R \qquad (16)$$

$$\bullet CH_3 + \overset{O}{\overset{\|}{HC}} \longrightarrow CH_4 + CO \qquad (17)$$

Being highly reactive, methyl radicals will combine with a variety of other substrates, so a stoichiometric relation between CO and CH_4 formation would not be expected.

The addition of sodium sulfite to remove oxygen reduced CO production more than was expected for zero oxygen concentration. One possible explanation is that the curves in Figure 19 have much steeper slopes as they approach zero than is shown. However, an alternate explanation consistent with the decarbonylation mechanism, involves the reaction of carbonyls with bisulfite (HSO_3-):

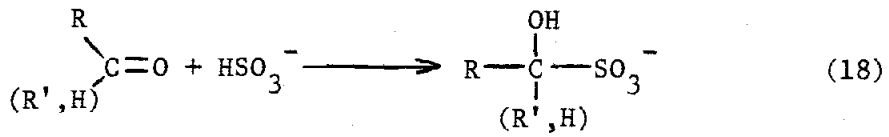

(18)

This reaction will occur with most aldehydes (at room temperature) but only with relatively unhindered ketones where R and R′ are small groups. The extent of this type of reaction in the seawater samples is therefore not known, but it would be unlikely for all carbonyl groups to be unhindered, and reactive. This would be especially true of humic matter.

The photochemical properties of the sulfite addition product are not known, but it seems reasonable to assume that generation of CO would be less likely since the pi bonding character of the carbonyl group is no longer present. (Bond cleavage results from transition of an electron to an anti-bonding pi orbital.) Therefore, the effect of sulfite on CO production supports the proposed decarbonylation mechanism, although it does not eliminate the possibility of other sources of CO.

Humic acid could be a significant source of photochemically produced CO. Carbonyl groups, and reactive precursors, are probably a significant portion of the chemical character of humic acid (Duursma, 1965). The complex bonding environment within the humic structure could make it possible for photochemical evolution of CO to be enhanced by lowering the energy required to result in bond cleavage. Unsaturated and aromatic structures may act as accessory pigments capable of absorbing light energy and subsequently

transferring this energy to reactive sites. The presence of metals or mineral phases may sensitize photochemical reactions as well as altering the electronic character of chelated carbonyl groups. Recall that mercury seemed to sensitize CO evolution.

Humic acid efficiently absorbs ultraviolet radiation in addition to short wave visible light. In constrast, acetone and acetaldehyde have UV absorption spectra with maxima at approximately 280 nm and 293 nm respectively (UV Atlas of Organic Compounds, 1966). The spectra overlap with the solar spectrum only from 290-320 nm. Lower absorbance over a narrow, low intensity portion of the solar spectrum for acetone and acetaldehyde versus high absorbance over a wide range for humic acid may account for the difference in CO production yields. Since cleavage of the carbon-carbonyl bond in simple compounds requires approximately 335 kJ mol^{-1} (radiation of 360 nm or less) carbonyl groups in marine organic matter, or humic acid, would have to be in environments that lower this energy threshold if CO production in the visible region is to take place. Given the complexity and metal content of marine humic material, this would seem possible.

A mechanism by which photooxidation of organic matter results directly in CO formation is not known, although, photooxidation can result in carbonyl formation. An example is addition of singlet oxygen across a carbon-carbon double bond (Foote, 1968):

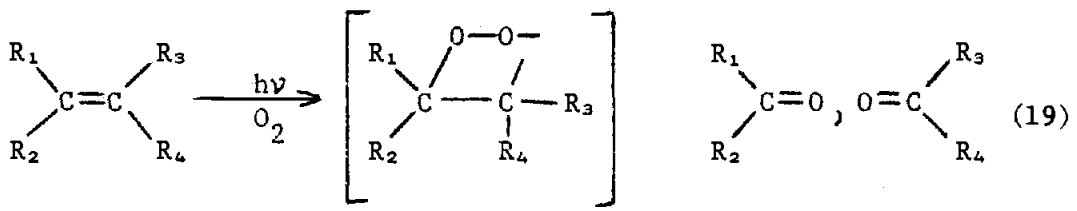

(19)

The two excited singlet states of oxygen are 22.5 and 37.5 kcal/mole above the triplet ground state. These energies correspond to wavelengths of 1271 nm and 763 nm. Therefore, in principle, there is sufficient energy throughout most of the visible spectrum to excite oxygen and result in oxidation of organic matter. Numerous organic triplet sensitizers exist which can enhance singlet oxygen formation, excitation by chlorophyll being one example.

VII. CONCLUSIONS

Some of the characteristics of photochemical production of CO have been experimentally determined and described in this work. This information is useful for developing an understanding of the observed oceanic distribution pattern of CO. In addition, it was possible to propose a possible photochemical mechanism for CO production which in turn relates to the influence of photochemical processes on the dissolved and particulate consituents of seawater.

The rate of CO production, for a given level of irradiance, was found to increase exponentially with shorter wavelength radiation and is maximized in the ultraviolet region. However, wavelengths as high as 500-600 nm seemed to have sufficient energy to produce measurable amounts of CO. These spectral characteristics are significant since seawater preferentially transmits light in this region throughout much of the euphotic zone. This must be taken into account when attempting to explain the extent of CO variations with varying light intensity within the water column. The spectral characteristics of CO production are also important when considering the energy requirements for known chemical transformations.

The production of CO in this study appeared to be a relatively fast photochemical reaction which contrasts with work from other investigators. Although maximum CO concentrations in surface ocean waters are found to lag behind maximum light intensities, a simple model was used to demonstrate that this observation is not inconsistent with instantaneous CO production.

One possible mechanism for production of CO is photo-decarbonylation of organic matter. This was shown to occur in seawater with added acetone and acetaldehyde although only for substrate concentrations that were high relative to the dissolved organic content of seawater. Carbon monoxide production from dissolved humic acid was much higher than from acetone or actaldehyde. If photo-decarbonylation occurs at wavelengths in the visible region (which were shown to produce CO in seawater) then carbonyl groups must be in chemical environments that effectively lower the activation energy required for bond cleavage. Production of carbonyl groups may occur concurrently by photooxidation of organic matter with dissolved oxygen.

BIBLIOGRAPHY

Baker, K. S., R. C. Smith, and A. E. S. Green. 1980. Middle ultraviolet radiation reaching the ocean surface. Photochem. Photobiol., 32: 367-374.

Bauer, K., R. Conrad, and W. Seiler. 1980. Photooxidative production of carbon monoxide by phototrophic microorganisms. Biochim. Biophys. Acta., 589: 46-55.

Bricaud, A., A. Morel, and L. Prieur. 1981. Absorption by dissolved organic matter of the sea (yellow substance) in the UV and visible domains. Limnol. Oceanog., 26: 43-53.

Broecker, W. S., and T.-H. Peng. 1974. Gas exchange rates between air and sea. Tellus, 26: 21-35.

Bullister, J. L., N. L. Guinasso, and D. R. Shink. 1981. Dissolved hydrogen, carbon monoxide, and methane at the CEPEX site. Ph.D. Thesis, Dept. of Oceanography, Texas A & M Univ., College Station, Texas.

Burris, R. H. 1979. p.569-604, Ch.5 In R. W. F. Hardy, R. Bottomley, and R. C. Burns (eds.), A treatise on dinitrogen fixation. Wiley, New York.

Calkins, J., and T. Thordardottir. 1980. The ecological significance of solar UV radiation on aquatic organisms. Nature, 283: 563-566.

Carlucci, A. F., S. B. Silbernagel, and P. M. McNally. 1965. Influence of temperatures and solar radiation on persistence of Vitamin B_{12}, Thiamine, and Biotin in seawater. J. Phycol., 5: 302-305.

Chappelle, E. W. 1962. Carbon monoxide oxidation by algae. Biochim. Biophys. Acta, 62: 45-62.

Conrad, R., and W. Seiler. 1980a. Photooxidative production and microbial consumption of carbon monoxide in seawater. FEMS Microbiol. Lett., 9: 61-64.

Conrad, R., and W. Seiler. 1980b. Role of Microorganisms in the consumption and production of atmospheric carbon monoxide by soil. Appl. Env. Microbiol., (1980): 437-445.

Conrad, R., W. Seiler, G. Bunse, and H. Giehl. 1982. Carbon monoxide in seawater. EOS 63: 527.

Corwin, J. F. 1970. Volatile organic materials in seawater, p. 169-180. In D. W. Hood (ed.), Organic matter in natural waters. Inst. Mar. Sci. Publication No.1, Alaska.

Coxon, J. M., and B. Halton. 1974. Organic photochemistry. Cambridge Univ. Press, Great Britain. 196 p.

Douglas, E. 1965. Solubilities of argon and nitrogen in seawater. J. Phys. Chem., 69(8): 2608-2610.

Duursma, E. K. 1965. The dissolved organic constituents of seawater, p. 433-475. In J. P. Riley, and G. Skirrow (eds.), Chemical Oceanography, v. 1. Academic Press, New York.

Ehhalt, D. H., and A. Volz. 1976. Coupling of the CH_4 with the H_2 and CO cycle: Isotopic evidence, p. 23-34. In H. G. Schlegel, G. Gottschalk, and N. Pfennig (eds.), Symposium on microbial production and utilization of gases (H_2, CH_4, CO). E. Goltze KG, Gottingen.

Ferenci, T., T. Strom, and J. R. Quayle. 1975. Oxidation of carbon monoxide and methane by Pseudomonas methanica . J. Gen. Microbiol., 91: 79.

Ferenci, T. 1976. The non-growth oxidation of carbon monoxide by Pseudomonas methanica and its relevance to studies of methane oxidation, p. 371-378. In H. G. Schlegel, G. Gottschalk, and N. Pfennig (eds.), Symposium on microbial production and utilization of gases (H_2, CH_4, CO). E. Goltze KG, Gottingen.

Foote, C. S. 1968. Mechanisms of photosensitized oxidation. Science, 162: 963-970.

Foreman, R. E. 1976. Physiological aspects of carbon monoxide production by the brown alga Nereocystis luetkeana . Can. J. Bot., 54: 352-360.

Green, E. J. and D. E. Carritt. 1967. New tables for oxygen saturation of seawater. J. Mar. Res., 25(2): 140-147.

Hannan, P. J., R. A. Lamontagne, J. W. Swinnerton, and C. Patoullet. 1977. Algae, ultraviolet light, and the production of trace gases. Nav. Res. Lab. Report ADA049441.

Hannan, P. J., J. W. Swinnerton, R. A. Lamontagne, and C. Patoullet. 1980. Effects of UV-B on algal growth rate and trace gas production, p. 177-190. In J. G. Eaton, P. R. Parrish, A. C. Hendricks (eds.), Aquatic Toxicology ASTM STP707

Hegeman, G. 1980. Oxidation of carbon monoxide by bacteria. Trends in Biochem. Sci., Oct.: 256-259.

Higgins, I. J., D. J. Best, and R. C. Hammond. 1980. New findings in methane utilizing bacteria highlight their importance in the bioshpere and their commercial potential. Nature, 286: 561-564.

Horspool, W. M. 1976. Aspects of organic photochemistry. Academic Press, London, 290 p.

Jerlov, N. G. 1968. Optical Oceanography. Elsevier, Amsterdam. 194 p.

Jerlov, N. G. 1976. Marine optics. Elsevier, Amsterdam. 231 p.

Junge, C., W. Seiler, U. Schmidt, R. Bock, K. D. Greese, F. Radler, and H. J. Ruger. 1972. Kohlenmonoxid-und wasserstoffproduktian mariner mikroorganismen im nahrmedium mit synthetischem seewasser. Naturwissenschaften, 59: 514-515.

Lamontagne, R. A., J. W. Swinnerton, V. J. Linnenbom. 1971. Nonequilibrium of carbon monoxide and methane at the air-sea interface. J. Geophys. Res., 76: 5117-5121.

Lilley, M., J. A. Baross, L. I. Gordon. 1982. Dissolved hydrogen and methane in Saanich Inlet, British Columbia. Deep Sea Research, in press.

Linnenbom, V. J., and J. W. Swinnerton. 1970. Low molecular weight hydrocarbons and carbon monoxide in seawater, p. 455-467. In D. W. Hood (ed.), Organic matter in natural waters. Inst. Mar. Sci. Publication No.1, Alaska.

Linnenbom, V. J., J. W. Swinnerton, R. A. Lamontagne. 1973. The ocean as a source for atmospheric carbon monoxide. J. Geophys. Res., 78: 5333.

Liss, P. S. 1973. Process of gas exchange across an air-water interface. Deep-Sea Res., 20: 221-238.

Liss, P. S., and P. G. Slater. 1974. Flux of gases across the air-sea interface. Nature, 247: 181-184.

Lorenzen, C. J. 1979. Ultraviolet radiation and phytoplankton photosynthesis. Limnol. Oceanog., 24: 1117-1120.

Lundgren, B., and Horjerslev, N. 1971. Daylight measurements in the Sargasso Sea. Kobenhavns Universitet, Rep. Inst. Fys. Oceanog., 14.

McCarthy, J. J. 1970. A urease method for urea in seawater. Limnol. Oceanog., 15: 309-313.

Meyer, O., and H. G. Schlegel. 1979. Oxidation of carbon monoxide in cell extracts of Pseudomonas carboxydovorans . J. Bacteriology, 137: 811-817.

Nozhevnikova, A. N., and L. N. Yurganov. 1978. Microbial aspects of regulating the carbon monoxide content in the earth's atmosphere, p. 203-245. In M. Alexander (ed.) Advances in microbial ecology, v. 2. Plenum Press, New York.

Pickwell, G. V. 1970. Physiology of carbon monoxide production by deep-sea coelenterates: causes and consequences. Ann. N.Y. Acad. Sci. 70, 174: 102-115.

Seiler, W., and C. Junge. 1970. Carbon monoxide in the atmosphere. J. Geophys. Res., 75: 2217-2226.

Seiler, W., and U. Schmidt. 1974. Dissolved nonconservative gases in seawater, p. 219-244. In E. D. Goldberg (ed.), The sea, v. 5. Wiley Interscience, New York.

Seiler, W., and U. Schmidt. 1976. The role of microbes in the cycle of atmospheric trace gases, especially of hydrogen and carbon monoxide, p. 35-46. In H. G. Schlegel, G. Gottschalk, and N. Pfennig (eds.), Symposium on microbial production and utilization of gases (H_2, CH_4, CO). E. Goltze KG, Gottingen.

Seiler, W. 1978. The influence of the biosphere on the atmospheric CO and H_2 cycles, p. 773-810. In W. E. Krumbein (ed.), Environmental biogeochemistry and geomicrobiology, v. 3. Ann Arbor Science, Michigan.

Sester, P. J., J. L. Bullister, N. L. Guinasso, and D. R. Shink. 1981. Continuous sampling of surface ocean waters off Southern California. submitted to Deep-Sea Res. 9-81.

Sevcik, J. 1976. Detectors in gas chromatography. 192 p. Elsevier, Amsterdam.

Smith, R. C., and K. S. Baker. 1979. Penetration of UV-B and biologically effective dose-rates in natural waters. Photochem. Photobiol., 29: 311-323.

Smith, R. C., K. S. Baker, O. Holm-Hansen, and R. Olsen. 1980. Photoinhibition of photosynthesis in natural waters. Photochem. Photobiol., 31: 585-592.

Smith, R. C., and K. S. Baker. 1981. Optical properties of the clearest natural waters. Applied optics, 20: 177-184.

Steemann Nielsen, E. 1974. Light and primary production, p. 361-414. In N. G. Jerlov, and E. Steemann Nielsen (eds.), Optical aspects of oceanography. Academic Press, New York.

Swinnerton, J. W., V. J. Linnenbom, and C. H. Cheek. 1968. A sensitive gas chromatographic method for determining carbon monoxide in seawater. Limnol. Oceanog., 13: 193-195.

Swinnerton, J. W., V. J. Linnenbom, and C. H. Cheek. 1969. Distribution of methane and carbon monoxide between the atmosphere and natural waters. Environ. Sci. Technol., 3: 836-838.

Swinnerton, J. W., V. J. Linnenbom, and R. A. Lamontagne. 1970a. The ocean: a natural source of carbon monoxide. Science, 167: 984-986.

Swinnerton, J. W., V. J. Linnenbom, and R. A. Lamontagne. 1970b. The distribution of carbon monoxide between the atmosphere and the oceans. Ann. N.Y. Acad. Sci. 70.

Swinnerton, J. W., and R. A. Lamontagne. 1974. Carbon monoxide in the southern Pacific Ocean. Tellus, 26: 136-142.

Swinnerton, J. W., R. A. Lamontagne, and W. D. Smith. 1976. Carbon monoxide concentrations in surface waters of the east tropical Pacific in 1974: comparison with earlier values. Marine Chem., 4: 57-65.

Uffen, R. L. 1976. Anaerobic growth of a rhodopseudomonas species in the dark with carbon monoxide as sole carbon and energy source. Proc. Nat. Acad. Sci. U.S.A., 73: 3298-3302.

UV Atlas of Organic Compounds. 1966. Plenum Press, New York.

Wiesenburg, D. A., and N. L. Guinasso, Jr. 1979. Equilibrium solubilities of methane, carbon monoxide, and hydrogen in water and seawater. J. Chem. Eng. Data, 24:356-360.

Wilkniss, P. E., E. B. Rodgers, J. W. Swinnerton, R. E. Larson, and R. A. Lamontagne. 1979. Trace gas concentrations, intertropical convergence, atmospheric fronts and ocean currents in the tropical Pacific. J. Geophys. Res. 84(c11): 7023-7033.

Wilson, D. F., J. W. Swinnerton, R. A. Lamontagne. 1970. Production of carbon monoxide and gaseous hydrocarbons in seawater: relation to dissolved organic carbon. Science, 168: 1577-1579.

Worrest, R. C., H. Van Dyke, and B. E. Thomson. 1978. Impact of enhanced simulated solar ultraviolet radiation upon a marine community. Photochem. Photobiol., 27: 471-478.

Worrest, R. C. 1981a. Impact of enhanced solar UV-B radiation upon marine phytoplankton: a position paper. Nat. Acad. Sci. Workshop on biological effects of increased solar ultraviolet radiation, Wash. D.C.

Worrest, R. C. 1981b. USEPA, Corvallis, Oregon, pers. comm.

Yagi, T. 1962. Enzyme oxidation of carbon monoxide. Biochim. Biophys. Acta, 30: 194-195.

Zafiriou, O. C. 1977. Marine organic photochemistry previewed. Marine Chem., 5: 497-522.

Zaneveld, J. R. V. 1975. Penetration of ultraviolet radiation into natural waters, p. 108-166. In Impacts of climatic change on the biosphere. Climate impact assesment program monograph 5, Sept. 1975.

Zavarzin, G. A., and Nozhevnikova, A. N. 1977. Aerobic carboxydobacteria. Microbiol. Ecol., 3: 305.

Zepp, R. G., and D. M. Cline. 1977. Rates of direct photolysis in aquatic environments. Env. Sci. Technol., 11: 359-366.

Zika, R. G. 1981. Marine organic photochemistry, p. 299-325. In E. K. Duursma, and R. Dawson (eds.), Marine organic photochemistry. Elsevier Sci. Pub. Co., New York.

APPENDIX

Stripping And Chromatographic System For Analysis Of Dissolved CO, H_2, CH_4, N_2O, N_2, and O_2+Ar In Aqueous Samples

A chromatographic system has been developed to analyse a suite of dissolved gases (CO, H_2, CH_4, N_2O, N_2, and O_2+Ar), in a single water sample. This system was designed to be compatible with the range of gas concentrations normally found in a variety of aquatic environments. The apparatus for stripping dissolved gases from a water sample, and the configuration of the gas chromatograph represent a synthesis of experience and information from previous designs which have been described in detail by Lilley et al. (1982). The system is summarized here and several modifications are explained which helped to simplify the operating procedure and adapt the stripping system to the experiments in this report.

In brief, water samples are transferred to a stripping system where a stream of dispersed helium extracts the dissolved gases by partitioning. Gases are carried to a liquid N_2 cooled Molecular Sieve 5A$^{(R)}$ (MS5A) trap where they are adsorbed and concentrated. After a period of time sufficient for quantitative extraction of gases from the sample (10 min.), the trap is heated to "inject" the gases into the chromatographic system where each gas is separated on MS5A columns which are at different temperatures, and then routed to appropriate detectors.

The salient feature of this system is the use of a single main trap to collect and concentrate all gases prior to analysis. This facilitated the use of a programmable integrator to automate the analysis (timing of valve switches, trap heating, and sequential detector signal processing). In earlier versions, a series of traps at different temperatures were used manually to separate and condense the different gases prior to analysis.

Analysis time for the present system is 19 minutes per sample, or 13 min. when samples are run continuously. A sample can be stripped while the previous sample is being chromatographed.

Gas Stripping and Standard Injection System

The apparatus used in these studies for stripping water samples of dissolved gases and injecting standard gas mixtures into the system has been described by Lilley et al. (1982). Only the method of introducing a water sample in line with the helium stream was changed since the quartz flasks used for irradiating samples were not adaptable to the original scheme.

Normally, a sample contained in a flask with two-way stopcocks on each end was attached to the system such that the sample could be drained into the stripping flask without exposure to air. In this work, a flask with three-way stopcocks on each end was mounted permanently in place of the sample flasks (see Figures 26 and 27). This flask was isolated by turning the stopcocks 1/8 turn which resulted in a positive helium pressure in the flask. By turning the bottom stopcock an additional 1/8 turn, the air in the siphon tube

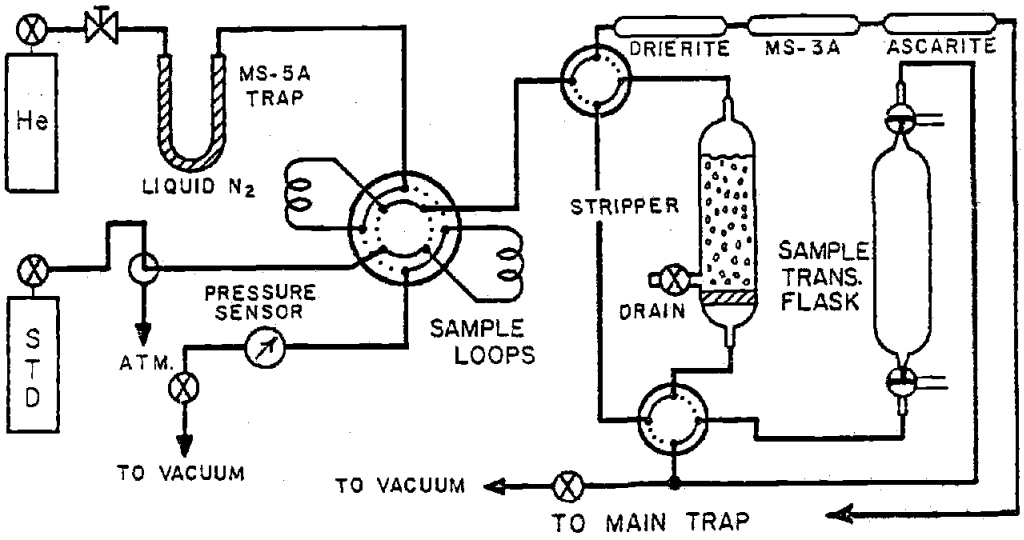

Fig. 26. Water sample stripping system showing position of the sample transfer flask.

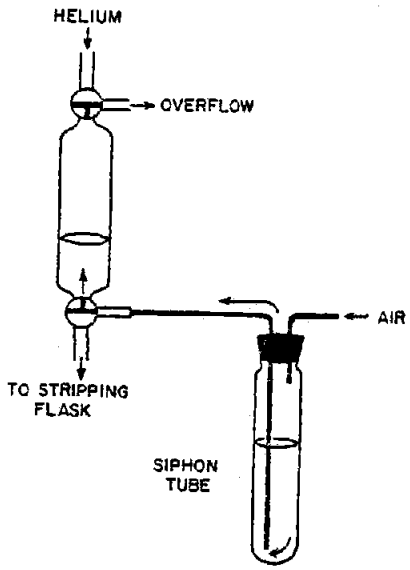

Fig. 27. Sample transfer flask and method of transferring water samples from quartz flasks.

attached to the lower side arm could be momentarily replaced by helium. The siphon tube was then quickly put into a quartz flask, the top three-way stopcock turned to overflow, and the sample pumped quickly and smoothly into the flask using a hand pump as shown. Nearly all the sample from the quartz flask was transfered, and each three-way stopcock was turned 1/8 turn to isolate the sample. From this point, the sample was drained to the stripping flask and stripped with a dispersed helium stream as usual. The entire transfer step would take less than 30 s.

Despite momentary exposure to air, the sample transfer step was considered acceptable for several reasons: 1) Samples that had previously been stripped of dissolved gases with N_2 showed no measurable concentrations of CO, H_2, O_2+Ar, or CH_4 when analysed by this method indicating contamination by air was not measurable. 2) "Worst case" calculations (that follow) based on the diffusion film model (Liss, 1973; Liss and Slater, 1974) indicate that diffusive loss of dissolved gases that were supersaturated should be minor during the transfer step.

The flux across an air-water interface is described by:

$$F = \frac{D\,dC}{z} \quad (\text{mole cm}^{-2}\text{s}^{-1})$$

If D, the molecular diffusion coefficient, is approximately $1.5\text{x}10^{-5}$ cm^2s^{-1} (Broecker and Peng, 1974), z, the stagnant film thickness, is .004 cm (Liss, 1973), and dC, the difference in concentration between the bulk solution and the atmospheric saturation concentration at the interface is maximized by assuming an atmospheric

saturation value of zero such that dC = concentration of the bulk solution, then a maximum loss of gas can be approximated.

The percent change in concentration (Δ) by this calculation is independent of the actual gas concentration, but dependent on the sample volume (155 cm^3) and surface area (7 cm^2).

$$\Delta\% = \frac{\text{moles of gas lost by diffusion}}{\text{moles of gas in sample}} \times 100$$

$$= \frac{D \times \text{area} \times 30\ s}{z \times 155\ cc} \times 100 = 0.5\ \%$$

Gas Chromatograph

A schematic diagram of the chromatographic system is shown in Figure 28, and Tables 12 and 13 list the individual components and normal operating conditions. Valves (V2,V3,V4) are shown in their initial orientations with the sample stream entering the system carrying stripped gases or a standard mixture of gases from the stipping apparatus entering the system. Valve switching and trap heating was done automatically using a Hewlett-Packard 3388 programmable integrator. Relay switches were used to supply power to valve motors and the trap heater.

An inexpensive and reliable method was developed to heat the main trap (Gordon, 1982, in preparation). The core from a 260/200 W soldering gun (Weller) was wound four times with 0.28 cm copper wire as a secondary coil. Brass swagelok tees (bored out to pass the trap tubing) were used to connect the terminals of the secondary coil to the stainless steel trap tubing, and a nylon union was used at one end of the trap for insulation. When operated at 70 V, the trap could be

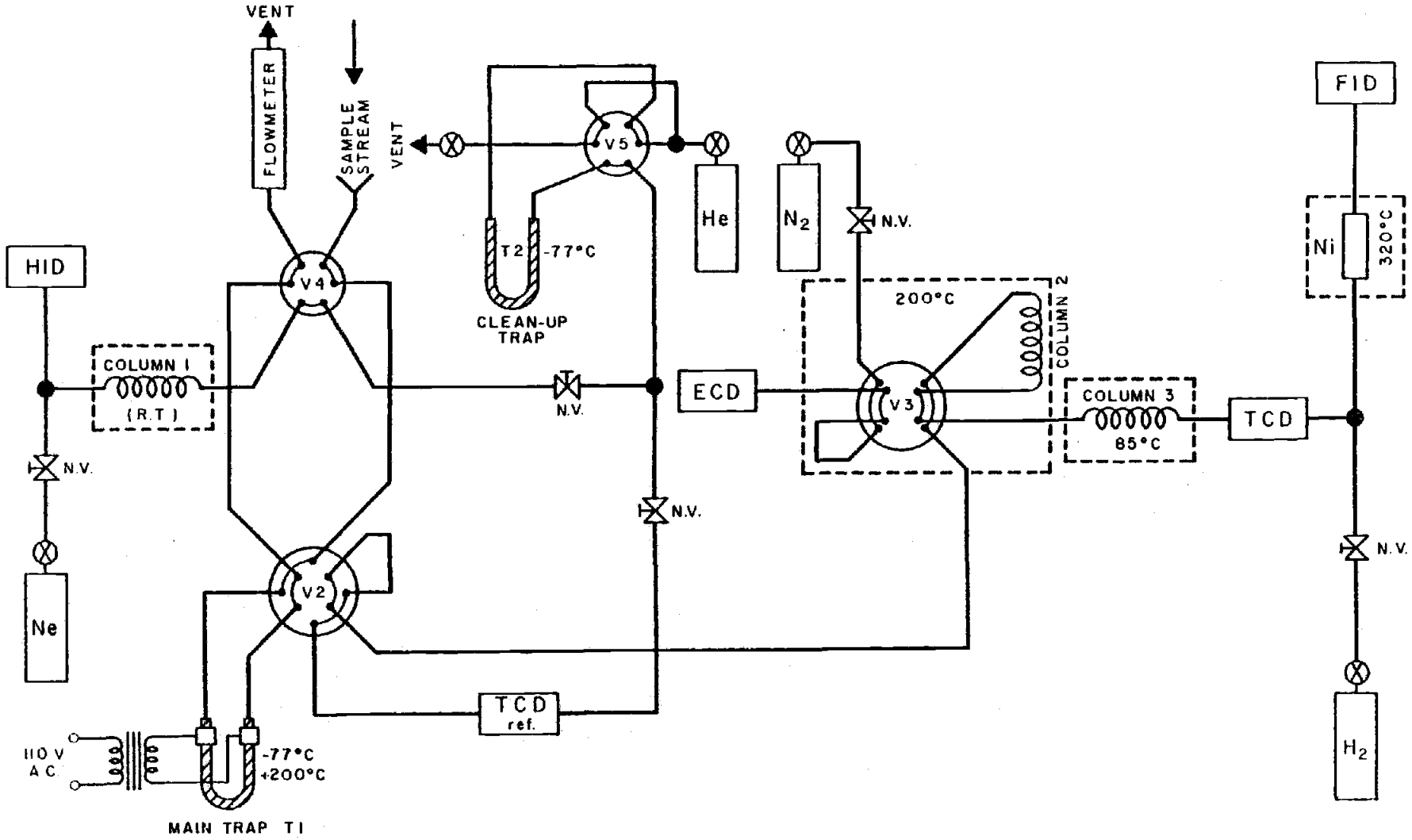

Fig. 28. Schematic of gas chromatographic system used for analysis of dissolved trace gases. Gases stripped from samples enter at "sample stream".

Table 12. Components of Gas Chromatograph

Tubing and Swagelok(R) fittings: stainless steel (3.18 mm in O.D. tubing has I.D.= 2.16 mm unless noted otherwise)

Coulmn 1: 2 m x 3.18 mm packed with 80/100 mesh Moecular Sieve MS5A(R)

Column 2: 60 cm x 3.18 mm packed with 80/100 mesh MS5A

Column 3: 2 m x 3.18 mm packed with 80/100 mesh MS5A

Nickel Catalyst (Ni) : 10 cm x 3.18 mm packed with nickel oxide on firebrick

V2: Carle 8 port microvolume valve

V3: Valco 8-port high temperature valve

V4, V5: Carle 6-port microvolume valve

Valve motors: Carle Valve Actuators

T1: Main Trap, 31 cm x 3.18 mm (2.54 mm I.D.) stainless steel. Middle 18 cm packed with 60/80 mesh MS5A and plugged with glass wool.

T2: Clean-up Trap, 45 cm x 6.35 mm O.D., packed with 60/80 mesh MS5A

N.V.: needle valves

HID: Helium ionization detector (Antek)

FID: Flame ionization detector (Fisher)

ECD: Electron capture detector (Analog Technology/Valco)

TCD: Thermal conductivity detector (Carle)

Table 13. Operating Conditions of Gas Chromatograph

Column temperatures:	Col. 1.....	room temperature
	Col. 2.....	200 C
	Col. 3.....	85 C
Detector temperatures:	HID.....	room temperature
	ECD.....	250 C
	FID.....	200 C
	TCD.....	120 C
Nickel Catalyst temperature:		320 C
Flow rates:	Col. 1, initial.....	28 ml/min
	Col. 1, Tl in line.....	26.5 ml/min
	Col. 2 and Col. 3 with He.....	28 ml/min
	Col. 2 with N_2.....	32 ml/min
	Col. 3 isolated from Col. 2...	26.5 ml/min

heated from room temperature to 200 C in 20 s. Only the portion of the trap between the terminal connections was heated. The brass connections remained at room temperature.

As shown, the sample stream initially flows through the MAIN TRAP, T1, which is immersed in liquid N_2, and all gases except helium are adsorbed and concentrated by the Molecular Sieve. After 10 min. the liquid N_2 is removed allowing the main trap to warm at room temperature and at the same time the valve switching/integration sequence is initiated. Valve 4 is immediately rotated which directs a carrier stream of helium through the main trap and into column 1. As the main trap warms, hydrogen is mobilized first and enters column 1. The function of column 1 is to provide enough time for the helium ionization detector (HID) signal to recover from flow upsets caused by switching valves before hydrogen enters. Once hydrogen has entered column 1, and before other gases are mobilized, V2 and V4 are simultaneously rotated and the main trap begins heating. This isolates the Column 1/HID section as hydrogen is being carried to the HID, and also directs a separate carrier stream of helium through the main trap and through columns 2 and 3. The trap reaches a temperature of about 200 C in 20 s. and the remaining gases are mobilized. After 2.5 minutes V2 is returned to its initial position and another sample may be stripped. Column 2 retards N_2O , separating it from the other gases, and Column 3 separates O_2+Ar, N_2, CH_4, and CO (in order of elution). Oxygen plus argon, and N_2 are detected by the thermal conductivity detector (TCD). Methane and carbon monoxide are detected by the flame ionization detector (FID). Carbon monoxide is reduced to methane by the nickel catalyst prior to entering the FID.

Finally, valve 3 is rotated to direct nitrous oxide (which is still in column 2) to the electron capture detector (ECD). At this point, N_2 replaces He as the carrier gas in column 2 and overtakes N_2O. As a carrier gas for the ECD, N_2 has a high ionization cross-section that helium does not. The ECD background current has time to stabilize before N_2O enters the detector. The entire analysis requires approximately 19 min., and samples may be stripped and analysed at 13 min. intervals (stripping and chromatography may be done concurrently). A summary of the sequence of operations is listed in Table 14. A sample chromatogram is shown in Figure 29.

Limits of detection are dependent on the sample volume, V_s, and the ability of the integrator to recognize and respond to a peak. The calculated limits based on the smallest detected peaks were 10 pmol/V_s for CO and CH_4, 5 pmol/V_s for H_2, and approximately 80 nmol/V_s for N_2 and O_2 (see note on calculation of O_2 concentrations). The linear range included the entire range of concentrations measured in this project.

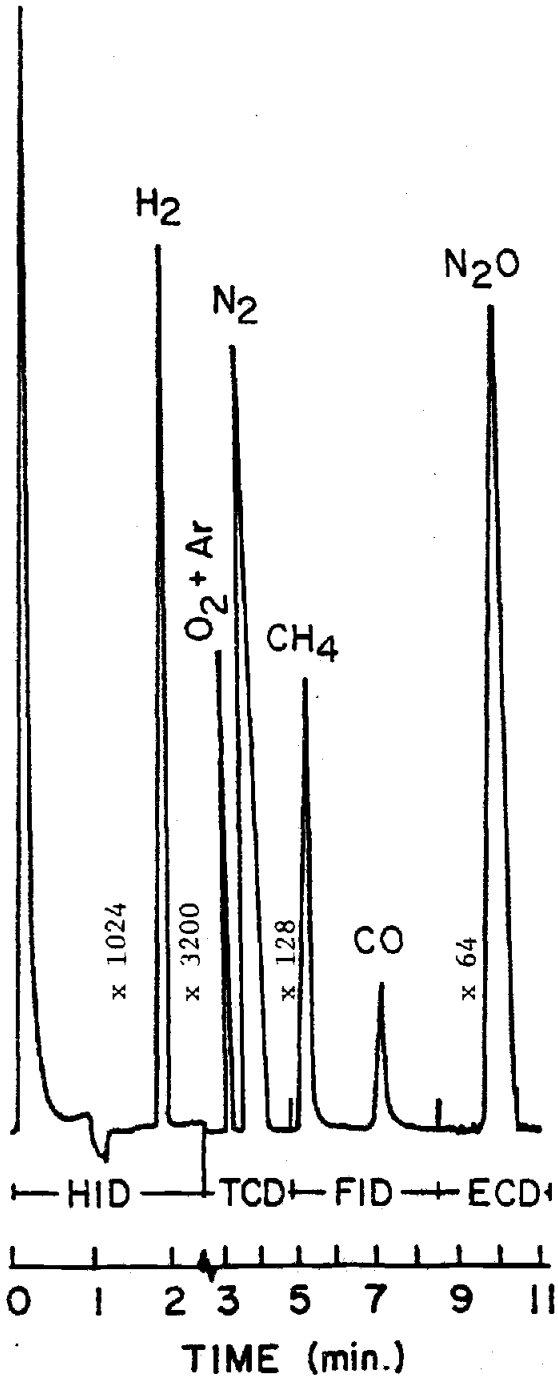

H_2: 1.03 nmol

O_2: 18.7 umol

Ar: 0.83 umol

N_2: 69.7 umol

CH_4: 2.26 nmol

CO: 1.06 nmol

N_2: 2.24 nmol

Fig. 29. Sample chromatogram.

Table 14. Operation sequence for gas chromatograph.

time (min)	Operation
0.01	HID signal reported
0.02	V4 rotated to direct carrier stream through trap to HID
0.03	Trap heater on
0.07	Trap heater off
0.83	V4 rotated to initial position
	V2 rotated to direct carrier stream to Column 2
	Trap heater on
2.46	TCD signal reported
2.47	V2 rotated to allow stripping of next sample
2.50	Trap heater off
4.71	FID signal reported
8.50	V3 rotated to direct N_2 carrier gas through column 2
	ECD signal reported
11.00	V3 rotated to original position
	End

Sample Calculation

1) Integrator counts for n blank runs averaged for each gas peak:

$$\text{Counts}_{i,blk} = \left(\sum_{x=1}^{n}(\text{Blank counts}_{i,x})\right)/n$$

2) Integrator counts for standard peak of gas (i) are made proportional to moles of gas (i) injected:

$$\text{Counts}_{i,prop.} = \frac{(\text{Counts}_{i,std} - \text{Counts}_{i,blk})}{(V,std)\left(\frac{P}{760\ mm}\right)\left(\frac{273.2}{273.2+T}\right)\left(\frac{\text{Conc}_{i,std}}{\text{Molar vol}_i}\right)}$$

$$= \frac{\text{Counts}_i}{\text{nmole}_i}$$

V,std = volume of standard gas mixture (ml), (sample loop volume)

P = pressure of standard gas mixture in sample loop (mm Hg)

T = temperature of sample loop (k)

$\text{Conc}_{i,std}$ = concentration of gas (i) in standard mixture (ppm)

Molar vol_i = molar volume of gas (i) at STP (l/mole)

3) Concentration of gas (i) in sample:

$$\text{Conc.}_i = \frac{(\text{Counts}_{i,smpl} - \text{Blank}_{i,avg})}{(\text{Counts}_{i,prop})(V,smpl)}$$

$\text{Counts}_{i,smpl}$ = integrator counts for peak i

V,smple = Volume of sample (l)

Note on Calculation of Oxygen Concentration

Determination of oxygen concentrations in air equilibrated seawater required a correction for argon which was not resolved from oxygen by the chromatographic system. As a first approximation it was assumed that the TCD response to O_2 and Ar was similar.

The TCD signal is related to the thermal conductivities (K) and specific heat capacities (C) of the carrier gas (c) and eluted gas (s) by:

$$\text{Signal} = \left(\frac{Ks}{B} - (Kc)A\right) + \left(Cs - Cc\right) v$$

where B and A are constants, $0 < A < 1 < B$, and v is the flow rate (Sevick, 1976). For a carrier gas with a large value of Kc and an inert, low molecular weight eluted gas, the signal is dominated by the thermal conductivity term and will be similar for gases with $Ks << Kc$. Since the thermal conductivities of O_2 and Ar (0.245, and 0.164 W cm^{-1} K^{-1} respectively) are both low relative to He (1.470 W cm^{-1} K^{-1}) the TCD response should be similar. The TCD response was also linear over the range of O_2 peak heights measured using room air as the standard. O_2 standard peaks were calculated by correcting the O_2 + Ar peak for the atmospheric concentration of Ar:

$$\text{Peak}(O_2+Ar) \times \left(\frac{C(O_2)}{C(O_2+Ar)}\right) \simeq \text{Peak}(O_2)$$

For samples that were purged with nitrogen, it was assumed that

Ar was removed and no correction was necessary for calculating the oxygen concentrations that were subsequently established by purging with O_2. It was also assumed that sodium sulfite quantitatively removed O_2 for the purpose of these experiments. Only air-equilibrated samples required correction for the presence of dissolved Ar. Using the solubilities of Ar (Douglas, 1965) and O_2 (Green and Carritt, 1967), the recorded peaks were corrected as described and the oxygen concentrations were calculated in the usual manner.